Schematization of shear strength

The influence of the schematization of shear strength on the macro-stability safety assessment

CIE5050-09: Additional Graduation Work

Mariska Naaktgeboren 5145244

Delft University of Technology

Waterschap Rivierenland

ARCADIS

TU Delft

Abstract

The Water Authority Rivierenland is responsible for periodically assessing the safety of the dike trajectories in the Alblasserwaard region. In 2012, the safety assessment for inner slope macro-stability was performed based on stress dependent design values for the shear strength, based on the cell test collection of the Water Authority. The most recent assessment on the inner slope macro-stability of the Lekdijk has shown a significant deviation from the previous assessment. According to these results, large scale reinforcement works are requested. Before starting any additional soil investigation, the water authority is interested in investigating the sensitivity of the schematization of the shear strength. The transition from the cell test collection to the triaxial and direct simple shear test collection, and therefore the transition from using the Mohr-Coulomb calculation model to the SHANSEP formulation, is expected to have the most impact on the outcome of the macro-stability safety assessment. The influence of the two test collections on the macro-stability safety assessment is analyzed by using a D-Geo-Stability model from the previous safety assessment for one cross-section of the Lekdijk, and transferring the model to D-Stability. The D-Stability model with the cell test collection parameters and the Mohr-Coulomb shear strength calculation model can be adjusted to the triaxial and direct simple shear test collection with SHANSEP shear strength calculation model. The transition from drained to undrained modelling results in a decrease of the shear strength of the soil around the failure surface. Therefore, the transition from the previous to the new test collection has resulted in a lower safety factor in the macro-stability analysis, having a negative impact on the overall macro-stability safety assessment.

Contents

Nomenclature

Abbreviations

Abbreviation	Definition
AGW	Additional Graduation Work
BOI	BeoordelingsInstrumentarium
CAU	Consolidated Anisotropic Undrained
CD	Consolidated Drained
CIU	Consolidated Isotropic Undrained
CPT	Cone Penetration Test
CRS	Constant Rate of Stain
CU	Consolidated Undrained
DSS	Direct Simple Shear
KIS	Dike reinforcement project from Kinderdijk to Schoonhovenseveer
LOR	Leidraad Ontwerpen van Rivierdijken
MC	Mohr-Coulomb
NC	Normally Consolidated
OC	Over Consolidated
OCR	Over Consolidation Ratio
POP	Pre-Overburden Pressure
SAFE	Dike reinforcement project Streefkerk, Ameide and Fort Everdingen
SHANSEP	Stress History And Normalized Soil Engineering Properties
UU	Undrained Unconsolidated
WBI	Wettelijk Beoordelingsinstrumentarium
WTI	Wettelijk ToetsInstrumentarium
WSRL	Waterschap Rivierenland

Symbols

Symbol	Definition	Unit
α	Angle of slice inclination	degrees
Δu_w	Excess pore water pressure	kPa
$\sigma(')$	(Effective) Stress	kPa
τ	Shear stress	kPa
ϕ'	Friction angle	degrees
θ	Volumetric water content	%
ε	Strain	%
γ	Volumetric weight	kN/m^3
c	Cohesion	kPa
e	Void ratio	-
F or SF	Safety Factor	-
m	Strength increase exponent	-
S	Shear strength ratio	[-]
S_u	Undrained shear strength	kPa
U	Degree of consolidation	%

1

Introduction

The Water Authority Rivierenland (WSRL) is responsible for periodically assessing the dike trajectories in the Alblasserwaard region. For years, the water authority has been responsible for analysing the stability of the dikes in this region and reinforcing dike trajectories if required. The procedure for assessing the inner slope macro-stability of a dike has changed significantly over the years. In the 1990's, the safety assessment was based on stress dependent design values for the shear strength based on the cell test collection of the water authority. The method for schematization of the shear strength of a dike has been adjusted over time to better approach realistic soil behaviour. The most recent assessment on the inner slope macro-stability of the Lekdijk has shown a significant deviation from the previous safety assessment. According to the results from this safety assessment, large scale reinforcement works are required. The Water Authority Rivierenland has given the assignment to Arcadis from which an Additional Graduation Work (AGW) and a master thesis project resulted, to investigate the largest influences behind the deviation in the safety assessment for inner slope macro-stability.

Before starting any additional soil investigation in the region, the WSRL is interested in investigating the sensitivity of the schematization of the shear strength in the macro-stability safety assessment. The research will focus on the uncertainties that have the largest negative influence on the inner slope macro-stability safety factor. During the additional graduation work, the two aspects that are expected to have a significant influence will be investigated. The transition from the Mohr-Coulomb shear strength calculation model to the SHANSEP formulation is known to have resulted in lower values for the safety factor. The transition from the cell test collection to the triaxial and direct simple shear test collection also influences the outcome of the safety assessment greatly. Other components that are also expected to have an influence on the results of the macro-stability assessment are investigated during the master thesis project.

1.1. Research questions

The main research question of the AGW report is:

How do the changes in schematizing the shear strength influence the macro-stability safety assessment for one cross-section of the Lekdijk in the Alblasserwaard?

The main research question is supported by a number of sub-questions to be able to provide an answer for the main research question:

1. How has process of modelling the inner slope macro-stability for the safety assessment changed over time?
    (a) What calculation model was and is used in the macro-stability safety assessment?
    (b) What are the main differences between the two most recent macro-stability safety assessments?

   (c) How can the two safety assessments be compared?

2. Which type of laboratory soil tests were used to determine the shear strength of the soil underneath the dike?

   (a) Which laboratory tests match the loading conditions of the dike cross-section?
   (b) How can the different soil laboratory tests be compared?

3. How can the two test collections be compared?

   (a) What is the influence of undrained modelling on the shear strength?

1.2. Approach

A literature study on the history of the Alblasserwaard is used to highlight the complex lithology and the reinforcement works that were executed in the past. The literature study also includes research into how the macro-stability safety assessment has changed over time. The largest changes should be highlighted during the literature study. After the literature study, both the macro-stability safety assessments should be investigated in more detail. The most recent safety assessment on the inner slope macro-stability of dike trajectory 16-2 was done by HKV in 2020. The previous safety assessment was performed in 2012 for preparation of the reinforcement project KIS. During this project, the Lekdijk was reinforced from Kinderdijk to Schoonhovenseveer. It is important to investigate how the calculation methods of assessing the macro-stability of a dike for both safety assessments to be able to directly compare the two. The approach is to isolate the components that influence the outcome of the assessment and to check the contribution to the safety factor in the macro-stability analysis.

A key component in this safety assessment is parameter determination. The two test collections that are used during the assessments are based on different type of laboratory soil tests, and should be compared to determine the influence of changing the test collections. A literature study will be performed on the type of soil laboratory tests which are used to set up these collections. The influence of changing the test collection can be checked by analysing the macro-stability for a dike cross-section by using both test collections strength parameters.

1.3. Scope

In order to limit the scope of the additional graduation work, only one cross-section of the Lekdijk will be considered: AW159.+190m positioned in dike trajectory 16-2. This cross-section represents the dike trajectory from dike pole AW158.+025m to AW162.+110m. The dike profile is not influenced by any external factors such as buildings or houses to simplify the assessment. Only the failure mode of inner slope macro-stability will be considered. For the master thesis project, more cross-sections in the Alblasserwaard region will be considered.

The focus of the report will be on the influence of the change in test collections, and therefore the change in laboratory testing and influence of this on the macro-stability safety assessment. Other components that also influence the safety assessment will be discussed in the master thesis. Only characteristic values in the test collection will be considered since the process of calculating the design values for multiple stages of the safety assessment has changed significantly over time. All calculations will only include characteristic values so the same safety level is considered. Also, only the Dutch safety standards to assess the macro-stability of a dike are considered.

2

Alblasserwaard

The Alblasserwaard is situated on the south-east side of the province of South-Holland in the Netherlands. This chapter describes the literature study on the Alblasserwaard region, including a general description of the area, the local lithology, and more detail on the Lekdijk cross-section AW159.+190m.

2.1. General description of the region

Figure 2.1 displays the total area under supervision of the water authority Rivierenland. The Alblasserwaard is situated on the west side of the purple section. In the Alblasserwaard, the polder system has been used for decades to regulate the water through the region year-round. In the west upper corner of the Alblasserwaard, the mill network of Kinderdijk is located which is a cultural heritage on the UNESCO list. [14]. During winters, precipitation and excess water requires to be removed from the Alblasserwaard, during summers water is required to be pumped into the area to prevent further subsidence. [16]

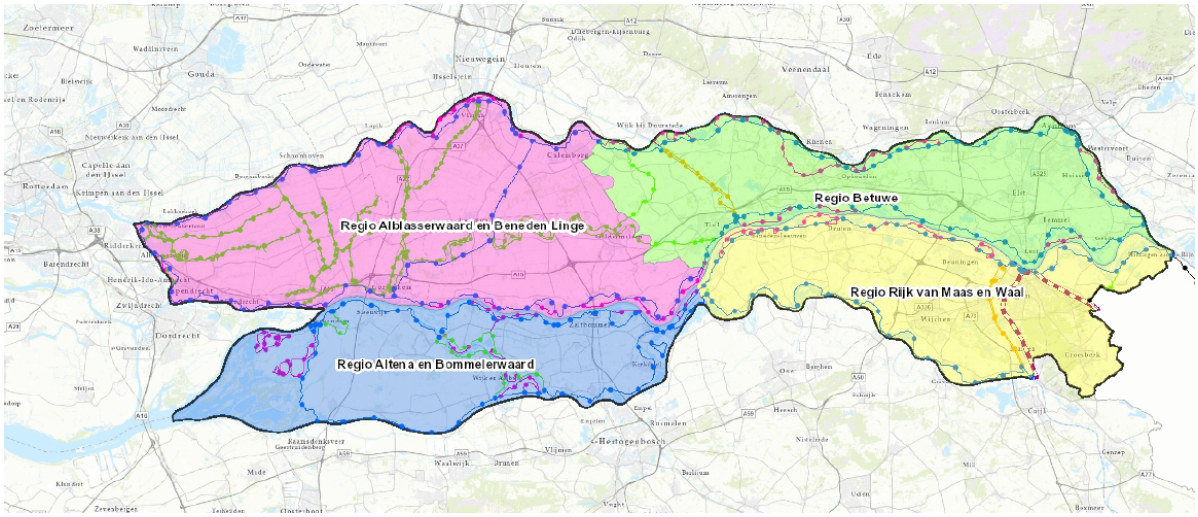

Figure 2.1: Management area of water authority Rivierenland, scale 1:342618 retrieved from GeoWeb

The Alblasserwaard is an interesting region since the lithology is complex and highly variable over the area. The Alblasserwaard nowadays is situated at around -1 to -2 m NAP while the subsoil consists of thick peat layers with clay. [16] The oxidation of peat is the largest contributor to the subsidence of the region, pared with the settlement of the soft soil layers. The dikes in this region are known to settle around 1 to 2 cm per year. The region is also filled with many sandy fluvial deposits of old riverbeds running through the peat layers, resulting in differential settlements. Instability issues of dikes in this region are not uncommon.

The river on the north side of the Alblasserwaard is the Lek and on the south side is the Merwede. The boundary between the Alblasserwaard and the Vijfheerenlanden is the Merwedekanaal running from north to south. The total length of all the dikes in the Alblasserwaard is 181.5 kilometer. The primary dike trajectory in the Alblasserwaard is classified as dike ring 16 which has a length of 85.6 kilometer. The primary dikes are shown by blue lines in figure 2.1 and the regional dikes are shown by green lines. Large sections of the primary and secondary dikes inner slope contain residential houses and monumental buildings. [16]

2.1.1. Dike profile AW159.+190m

The dike cross-section that is of interest for the AGW is located on the north side of the cultural heritage Kinderdijk and visible in figure 2.2. On the inner slope of the dike, the area is appointed as Natura2000. The dike profile is part of the Lekdijk, which is part of the primary flood defence system of the Alblasserwaard. The dike profile represents the dike section from AW158.+025m to AW162.+110m as can be seen in figure 2.2 in light pink. The color represents the national assessment for primary dike trajectories: the dike trajectory possibly suffices the lower boundary value set for the safety requirements. The orange color describes that currently, the dike does not comply with the set lower boundary, and the yellow section does suffice. These colors represent the current safety assessment which is built up from different failure requirements such as a crest height requirement, piping resistance, heave and macro-stability for the inner and outer slope. Currently, the dike section does not comply with the norm for inner slope macro-stability.

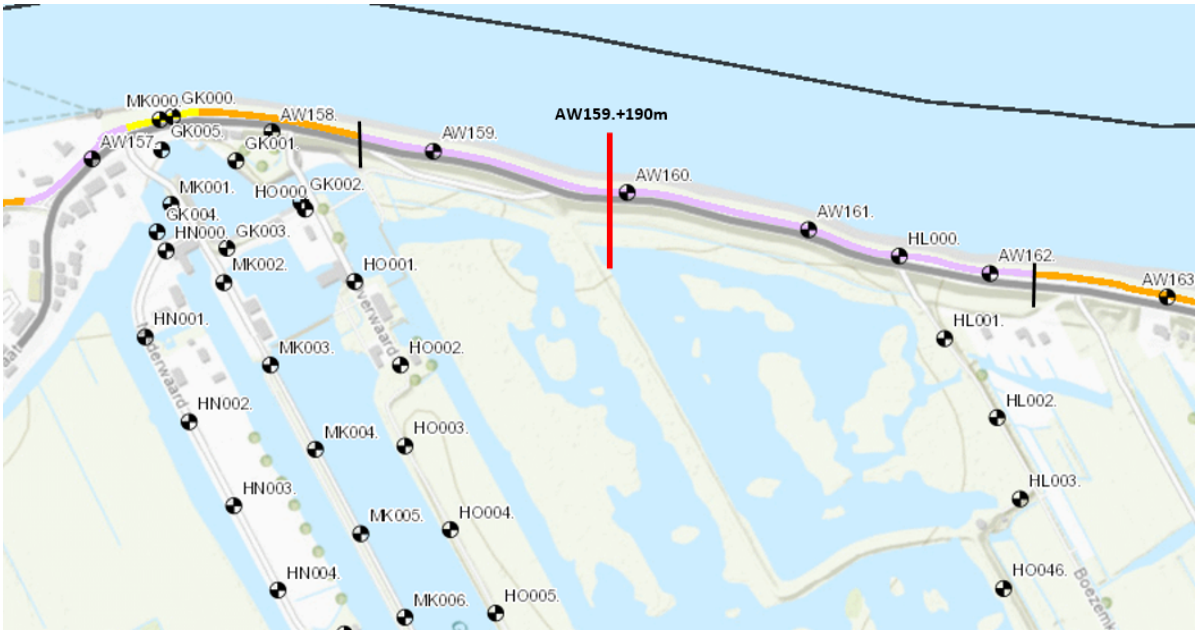

Figure 2.2: Location of cross-section AW159.+190 on the Lekdijk in the Alblasserwaard, scale 1:6000 retrieved from GeoWeb

2.1.2. Local lithology

The lithology of the Alblasserwaard is complex and highly variable over the area. Appendix A displays the extrapolated length profile of the local lithology based on CPT data. For cross-section AW159.+190m, the top layers between +5 and -5m NAP are anthropogenic soils which are not naturally deposited but were deposited during previous reinforcement works which will be discussed later in this chapter. The separation in reinforcement material is made between OA and OB to separate new and previously applied dike reinforcement material. The dike material is situated directly on top of the soft soil layers. These layers contain clay material interlayered with peat and vary in thickness.

Figure 2.3 displays the schematization of the subsoil of dike profile AW159.+190m that is used in the previous safety assessment for the macro-stability calculations. The separation in the subsoil is

made between underneath the dike (O) and next to the dike (N). This classification originates from the cell testing that was done for the scheduled reinforcement works in the 1980's. From the test results, it became visible that there was a significant difference in the strength parameters underneath the dike and next to it. The boundary for the classification of (O) under the dike is equal to 2/3 of the inner slope width from the crest.

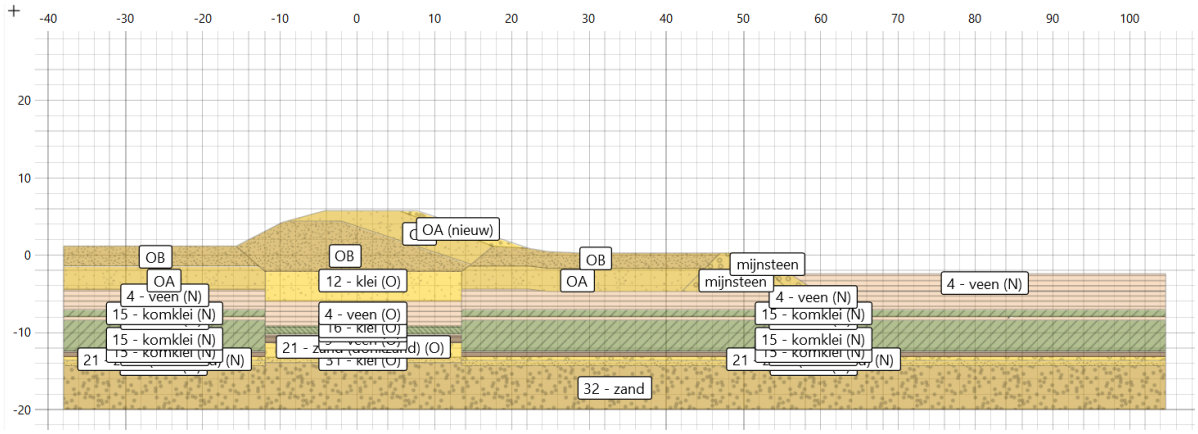

Figure 2.3: Dike profile AW159.+190m as simulated in D-Stability

Soil name	Description	WBI notation
OA	Anthropogenic sand soil	Dike material
OB	Anthropogenic clay soil	Dike material
OA new	Anthropogenic sand soil	Dike material
Mijnsteen	Anthropogenic sand soil	Dike material
4. Hollandveen	Peat	H_Vhv_v
9. Basisveen	Compacted peat	H_Vbv_v
12. Tiel klei	Silty clay with thin sand layers	H_Ro_z&k_k
15. Gorkum klei licht	Alteration peat and clay layers	H_Rk_k&v
16. Gorkum klei zwaar	Sandy clay to clayey sand	H_Ro_z&k
21. Donkzand	Medium sand	P_Wrd_zm
31. Kreftenheye klei	Silty sandy clay	P_Rk_k&s
32. Pleistoceen zand	Fine to medium sand	P_Rg_zm

Table 2.1: Soil classification and notation [8]

Table 2.1 displays all soil types which are used in the schematization of the dike profile shown in figure 2.3. These soils are also included in the test collections which will be discussed in chapter 4.

2.2. Reinforcement projects

Around 1980, reinforcement works on the primary dike trajectory 16 were executed by adding material to widen the dike and add height to the crest. The reinforced dike profiles were designed without taking the mechanism uplift of the blanket layer behind the dike into consideration.

During the 90's, the macro-safety assessment started taking the uplift mechanism into consideration and sections of the dike trajectory did not suffice to the safety standard. For these dike sections, the berms on the inner slope were considered too short. These sections of the dike trajectory were reinforced again. If possible, the inner berms were extended into the hinterland. The inner berm was placed at the dike AW159.+190m with the 'mijnsteen' material in order to keep the inner berm in place, visible in figure 2.3. For sections of the dike trajectory where this extension was not possible, constructions were applied such as concrete sheet piles at the inner toe to increase stability and reduce groundwater flow. [1]

The next round of reinforcement works on the Lekdijk started in 2013 from Kinderdijk to Schoonhovenseveer (KIS). The project was conducted from west to east and finished around 2018. The reinforcement works on the dike trajectory were based on the previous safety standards and the dike material 'OA nieuw' was added to the dike to widen the crest. The inner slope of the dike was shifted, as well as the road to create space for a bicycle lane on the river side of the dike.

In the most recent safety assessment for dike trajectory 16-2, a strict calculation guideline on macro-stability is applied. The calculation method for the shear strength of the dike material has been adjusted since the previous safety assessment done for the KIS reinforcement project, which will be discussed in more detail in chapter 3. It is noticeable for dike trajectory 16-2, that the majority of the dikes that are reinforced in an equivalent way as AW159.+190m, the new assessment signals the macro-stability as 'possibly suffices'.

A new reinforcement project is scheduled for 2025, the SAFE project on dike trajectories 16-3 and 16-4 from Streefkerk to Fort Everdingen. The reinforcement works will focus on increasing stability and preventing piping.

3

Macro-stability safety assessment

Riverdikes are exposed to high water levels relatively long, so the focus in the stability assessment of riverdikes is on the failure mechanisms that are likely to occur due to high water levels: water overflow, wave overtopping, piping and sliding of the inner slope. [12] The failure modes for high water levels are shown in figure 3.1. The sliding of the inner slope is also known as macro-stability: which describes the ability of the dike to resist a variation in loading conditions without loosing its function. Since only primary dikes are considered, the function of the dike can be described as the retainment of the river water. The failure mode macro-stability can occur when the strength of the dike is not sufficient to resist the loading conditions. This may result in a shear failure of soil which can occur along straight or a circular slip surface. [10] If the soil is saturated, the risk of macro-instability will increase. If the soil is dry, the soil is compacted and less likely to fail on due to inner slope instability.

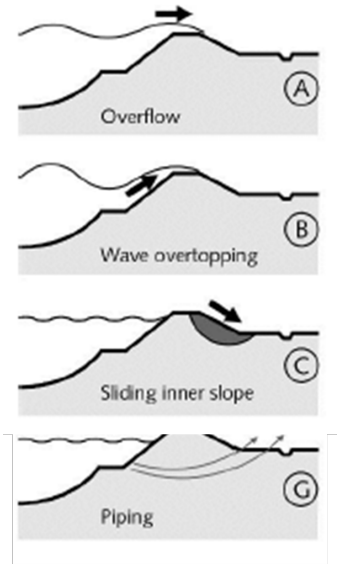

Figure 3.1: Riverdike failure mechanisms [4]

The height of the crest of the dike is the primary element that determines the ability to retain water, since it can be translated directly to a probability of flooding and overflowing. Other elements of a dike profile can be applied to support the crest height and avoid large deformations for varying loading conditions. If the crest fails, the infiltrating water could lead to erosion of the dike material and instability issues. Dike elements that mainly influence the macro-stability of the inner dike slope are the crest height, the dike core material, the steepness of the inner slope, presence of an inner berm or ditch and potential drainage solutions. [10]

The calculation method to analyse the macro-stability of a dike profile that is used in the Netherlands has changed gradually over time. However, the essence of the calculations is still the same: to determine the resisting force provided by the soil and the driving force resulting from the loading conditions to calculate the most critical failure surface.

3.1. Approach 1980's

Dike reinforcement projects before 1980 were mostly based on experience and knowledge gained throughout the years. From these experiences and knowledge, the 'leidraden' for rivers in the north part of the Netherlands (LOR1) were set up in 1985 and for the southern rivers of the country in 1989. The 'leidraden' are used in the Netherlands as a standard to calculate the macro-stability of primary riverdike

trajectories. The reports describe simple procedures for aspects such as the process of schematizing the subsoil, calculating the design values of high-water levels and indicating the macro-stability of the inner and outer slope of a dike. The calculation of the safety factor for the shearing of the dike material, was done by one of the following methods: [12]

- Using the momentum balance equation for each point in the soil and checking the stability by using finite element method.
- Indicating the most critical slip plane and use the momentum balance equation around the failure plane.

The finite element method was expensive at the time and complex, so this was only used for special situations. The routine assessment of the macro-stability for dike trajectories was done with a simplified slip circle calculation. Entire dike trajectories were split up into multiple sections, where one dike profile would be fixed to be the most critical and represent the entire trajectory. The slip surface calculations are modelled in 2D and calculated with Bishop's simplified method, of which an example is shown in figure 3.2. Bishop's method is still used nowadays to iteratively determine the most critical slip circle to provide a safety factor for the macro-stability of a dike cross-section.

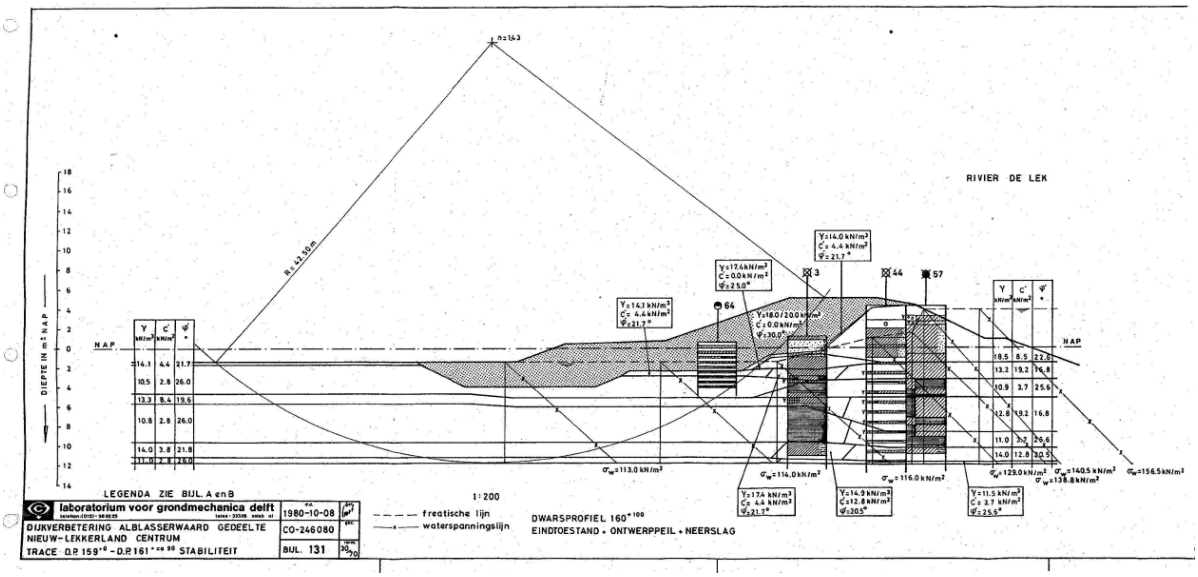

Figure 3.2: Bishop calculation for the reinforcement works on the Lekdijk in 1980

Bishop's formulation that is used to calculate the safety factor per slice of the slip circle is shown in equation 3.1 [15]. The formula includes the driving forces resulting from the self weight of the soil body and compares this to the resisting moment of the soil. [9] The formula is used to determine the safety factor *F*, which provides a value on the stability of the slope. The input parameters for the Bishop formulation can be obtained from soil laboratory tests and is discussed in Chapter 4.

$$F = \frac{\sum \frac{c+(\gamma h - p)\tan\phi}{\cos\alpha(1+\tan\alpha\tan\phi/F)}}{\sum \gamma h \sin\alpha} \tag{3.1}$$

The maximum resisting moment occurs if the soil at the failure surface has reached the maximum shear stress. The shear stress can be calculated by using the Mohr-Coulomb failure criterion, shown in equation 3.2.

$$\tau = c + \sigma_n \tan\phi \tag{3.2}$$

The 'leidraden' also describe the safety standard for macro-stability during this time. The minimum allowable safety factor (F_{min}) from the Bishop analysis for a riverdike profile was set to 1.3. The safety factor from the Bishop calculation shown in figure 3.2 for the reinforced Lekdijk was equal to 1.40.

3.2. Approach 1990's

The LOR2 is set up in the 1990's to extend LOR1. The calculation methods of the macro-stability of dikes was extended with the Uplift calculation method. This method is beneficial since it separates the slip plane into an active, passive and horizontal section. The active and passive section can be described with two circles, where the horizontal section bounds the two. This model takes the influence of uplift of the blanket layer by the water pressure in the aquifer below the dike into consideration. The safety factor is calculated by taking the equilibrium of the slices and comparing the driving force and resistance of the soil. [6]

The LOR2 was also extended to include the process description for a semi-probabilistic calculation method to assess the macro-stability. The LOR2 also includes the use of a damage factor to account for the dependence of the stability with respect to the dike ring. For the Alblasserwaard region the damage factor was equal to 1.17. The transition from average values to the design value for the shear strength was also now included in the 'leidraden'. The statistical approach has been adjusted, as well as the model factors for both calculation methods.

3.3. Approach 2000's

With the introduction of the WTI ('Wettelijk ToetsInstrumentarium'), a new safety standard to approach the macro-stability safety assessment is initiated. The previous safety standards of the 'leidraden' describe the failure of a primary dike as exceeding the critical hydraulic boundary conditions. Previously, the structure was required that during design conditions the dike would still fulfill all requirements. Deformations and damages to the dike structure were limited, with only allowing 2% deformation during design conditions for macro-stability. The new safety standard of the WTI describes the failure related to the probability of flooding. With this innovative approach, the actual flooding and or breaching probability is calculated for each dike trajectory. [4]

3.4. Approach 2010's

The WTI documents were the set up for the upcoming WBI program, 'Wettelijk BeoordelingsInstrumentarium' which was introduced in 2017. In relation to the macro-stability calculations, the WBI switched to using a simple test to indicate the general condition of any dike. If the stability was not sufficiently tested, a detailed test could be done if required. The WBI describes many factors that should be taken into consideration during the inner slope macro-stability assessment:

- Schematization of the dike geometry
- Parameter determination
- Loading conditions
- Hydraulic boundary conditions
- Statistic analysis to determine design values
- Sensitivity analysis

KIS reinforcement

The WTI and WBI were both used during the KIS reinforcement project. Since the project was executed from east to west, some sections (mostly on the east side of dike trajectory 16) are evaluated by using the WTI and sections the west side are evaluated using the WBI. For the dike section between AW158.+025m to AW162.+110m the WTI was used. The inner slope macro-stability was re-evaluated by using Bishop and Uplift to determine the effect of the new reinforced dike profile. The minimum safety factor for macro-stability was based on an exceedance probability of 1/2000, and was equal to 1.17 for the Bishop calculation and 1.23 for UpliftVan calculation. The Bishop safety factor was calculated to be 1.56 for the new reinforced dike. From the UpliftVan calculation model, shown in figure 3.3, the safety factor was equal to 1.31.

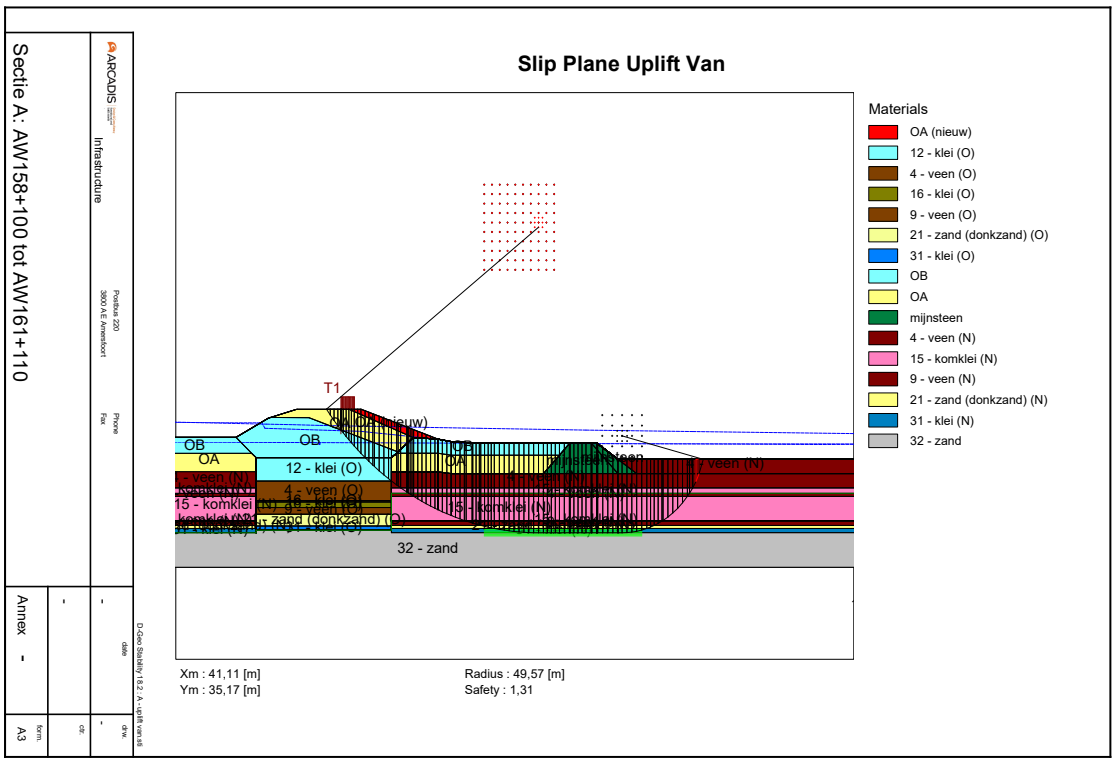

Figure 3.3: Results Uplift calculation AW158.+025m to AW162.+110m

SHANSEP

A major change in the calculation method described in the WBI was the introduction of the SHANSEP formulation, which could be used to approach the undrained shear strength of soft soils. Note that this calculation model for dike section between AW158.+025m to AW162.+110m8 was not implemented yet in the previous safety assessment. The subsoil in the Alblasserwaard region consist of thick impermeable peat and clay layers. The modelling of the shear strength of the soft soils will be more realistic if the undrained shear strength is used during the stability calculation. In the WBI, the SHANSEP formulation is described to calculate the undrained shear strength. In D-Stability, the SHANSEP formulation requires two material properties and one state parameter, as can be seen in equation 3.3. The parameters used in the formulation will be discussed in detail in chapter 4. The values for S and m can initially be approached by a standard value described in the WBI. [8]

$$S_u = \sigma'_v * S * OCR^m \tag{3.3}$$

Whether to simulate the soil behaviour drained or undrained during the macro-stability assessment is described in the WBI. Whether a soil behaves drained or undrained mainly depends on the soil type and the consolidation time of the soil. If the drainage length of a soil is small, a clay soil can still behave drained. If the drainage length is large, a sandy soil can still behave undrained. Usually, under the phreatic level, the soft soils are modelled as undrained with SHANSEP and the sand soils are modelled as drained with MC. For thin soil layers however, the behaviour can be modelled differently. [13]

3.5. Approach 2020's

New calculation methods that are added on to the WBI from 2017 can be found in the new BOI program. The most recent safety assessment of dike trajectory 16 started in 2020 and implements this program.

A new safety standard categorises the minimum factor of safety for macro-stability in six categories, as shown in table 3.1. The factors of safety are specified for the dike trajectory 16-2, since the safety factor now also depends on a failure probability which is assigned per trajectory.

Assessment	**Description**	**Required safety factor for inner slope macro-stability**
I_v	Exceeds the signal value	≥ 1.39
II_v	Meets the signal value	$1.30 \leq SF < 1.39$
III_v	Possibly meets the signal value, definitely meets the lower limit	$1.26 \leq SF < 1.30$
IV_v	Possibly meets the lower limit	$1.07 \leq SF < 1.26$
V_v	Does not meet the lower limit	$0.93 \leq SF < 1.07$
VI_v	By no means meet the lower limit	$SF < 0.93$

Table 3.1: Safety factors for macro-stability of recent safety assessment

The most recent safety assessment on the cross-section resulted in a classification assessment IV_v for the dike section between dike poles AW158.+025m to AW162.+110m8, as seen in figure 2.2 indicated by the light pink color. This displays a decrease in safety factor of at least 0.3 between the two safety assessments, from 1.56 to 1.26.

4

Soil laboratory testing

Laboratory testing is an important aspect in soil parameter determination. The execution of reliable laboratory tests is required to obtain realistic values for the shear strength of different soil types. Many laboratory tests were performed over the years on the soils in the Alblasserwaard, from which the WSRL created a test collection ('proevenverzameling'). This collection of laboratory test results is common among all the water authorities in the Netherlands. This data is especially useful in any type of research into the subsoil.

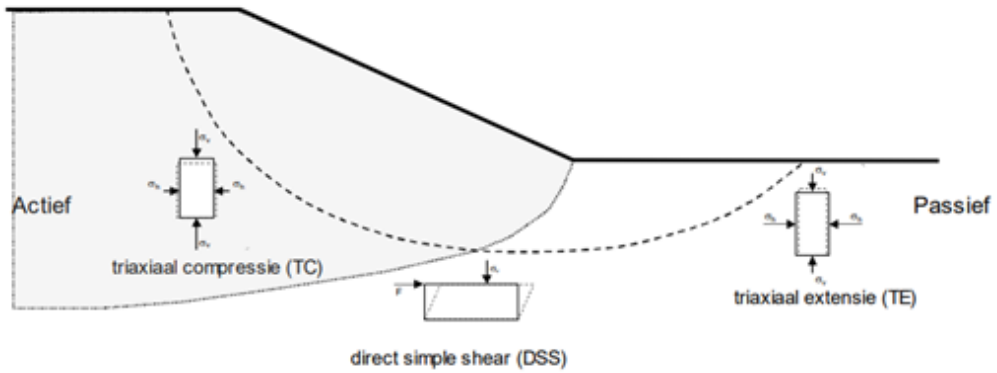

Figure 4.1: ADP method for laboratory test locations [8]

Figure 4.1 displays how, in theory, each laboratory test can be linked to the loading conditions of the inner slope of a dike profile by taking the macro-stability into account. Underneath the crest of the dike, the forces acting on this section of the slip circle can be simulated by a triaxial compression test. A triaxial extension test can represent the loading conditions in the hinterland, and a direct simple shear (DSS) test can be used to simulate the loading conditions at the horizontal section of the slip circle. [11] In practice, the approach of performing laboratory tests is not depended on location but soil related. The DSS test with constant height is only used on peat soils to simulate undrained conditions. A single stage triaxial consolidated undrained compression test (CAU) is used on soft soils. Triaxial tests cannot be used on peat samples and is also not used for sand samples. Usually, an assumption is made on the strength parameters of sand. The most critical section of the slip circle is the active part.

4.1. Cell testing

As preparation for the dike reinforcement works on the Lekdijk in 1981, the subsoil of the Lekdijk was investigated thoroughly by CPT's and borings. From the borings, soil samples could be extracted and used for laboratory cell testing. The cell test (or also known as Dutch cell test) was used to determine soil strength properties for a set of loading conditions which are comparable to the in-situ conditions of the soil. The schematic view of the test apparatus is shown in figure 4.2. The protocols for cell testing that is considered was documented in 1988, since the cell test is no longer used. The soil sample is enclosed by a porous stone at the top and bottom of the sample to allow for drainage. The soil sample is enclosed by a membrane, while the horizontal stress on the sample can be applied by the cell pressure. [11]

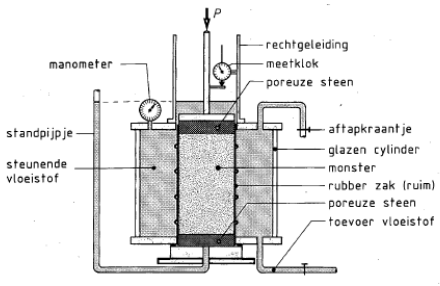

Figure 4.2: Schematic view of the cell test apparatus [11]

During the first stage of the cell test, the soil sample is loaded by the cell pressure, the sample will consolidate by lowering this pressure. Note that during this phase, the deviator stress is still present in the soil sample resulting in anisotropic consolidation. A stress rate of 0.01 mm per hour is assumed to be critical, so the end of consolidation phase is reached when the deformation of the sample is lower than this rate. The cell test was often performed as a multistage test, where the next stages are composed of critical stress combinations which are used to determine the shear strength of the material. A value for the cohesion (c) and friction angle (ϕ) can be calculated. For each stage, a maximum of 5 mm of vertical deformation was allowed. The downside to the multistage test is that the sample continues to deform throughout each stage, while for each new stage the assumption is made that the conditions are matching the in-situ stress. This can cause skewed results for c, ϕ and the shear strength of the soil.

Cell test	
Measurements before testing	A, γ_{sat}, θ
Measurements during testing	σ_3 , ε
Measurements after testing	ΔV, σ_1, A, γ_{sat}, θ
Calculated parameters	c, ϕ

Table 4.1: Parameters measured before, during and after cell testing

Table 4.1 displays a summary of the soil parameters that result from cell testing. Before testing, it is important to measure the dimensions of the soil sample, including the water content to measure the volume change of the soil after the test. The total test time of a cell test could take up 3 to 5 weeks due to the multistage testing, depending on the soil type. The results of the cell test are presented in a $\sigma - \tau$ diagram with the resulting critical stress circles per stage. The stress points are taken at a strain level of 2 to 5%. [11]

4.2. Triaxial testing

The cell test is the precursor of the triaxial test, the similarities between the two soil laboratory tests are visible in the schematic sketches of both test apparatus in figures 4.2 and 4.3. The soil sample in the triaxial test is restrained at the bottom and top of the sample with a porous stone, so any water in the sample can drain and the pore pressures can be measured if required. The soil sample in the triaxial test can be compressed or extended, depending on the loading requirements. The triaxial test works by restraining the stress or deformation of the soil sample to provide soil strength parameters. [11]

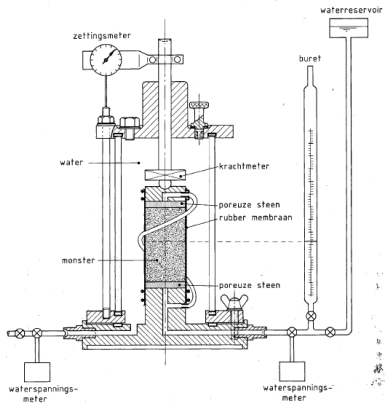

Figure 4.3: Schematic view of the triaxial test [11]

A protocol for performing triaxial tests is provided by Deltares from 2016 for obtaining consistent soil strength parameters. [3] With the previously used cell tests, there where no protocols set in place, so multiple laboratories would perform the tests in a different way. A number of requirements are that the sample of the triaxial test should meet is a height/-diameter ratio requirement of 1.8 to 2.2. The minimum diameter of the soil sample should be 50 millimeter.

The consolidation time of the soil sample is limited to three days, where the process is assumed to be completed when the pore pressure in the sample (resulting from closing drainage) do not increase more than 1 kPa in 10 minutes. The rate of testing depends on the test requirements. Triaxial tests are done multiple times on different samples from the same soil type to determine the average value for ϕ and its standard deviation. The friction angle is calculated at critical state, which the soil sample is assumed to have reached around 25% strain. the cohesion is assumed to be zero. [7]

Triaxial test	
Measurements before testing	A, θ, e
Measurements during testing	ε, σ_3, Δu_w, p', q, σ_v, τ or S_u
Measurements after testing	ΔV
Calculated parameters	c, ϕ, OCR, S, m

Table 4.2: Parameters measured before, during and after triaxial testing [15]

Table 4.2 displays a summary of the parameters used during triaxial testing. It is important to document the sample dimensions before and after testing to determine the volume change. The end of the consolidation process is assumed to be at a consolidation degree of $U = 95\%$, which mostly depends on the height and diameter of the soil sample and consolidation coefficient. Triaxial tests are used to determine the undrained shear strength ratio S which is used in the SHANSEP formulation as described in chapter 3. The ratio is calculated by the undrained shear strength divided over the consolidation stress gained from the triaxial tests. [8]

4.2.1. Type of triaxial tests

The triaxial test can be adjusted to match the in-situ conditions of the soil sample. The three most common of triaxial tests are listed below.

1. Unconsolidated undrained (UU)
   In the UU triaxial test, the soil sample is first loaded with the cell pressure. Directly after reaching the requested cell pressure, the sample is loaded vertically until failure without allowing drainage under constant cell pressure. The test provides the undrained shear strength S_u of the soil sample. The UU triaxial test is useful for soil types with low permeability to determine the undrained shear resistance of the soil. [11]
2. Consolidated undrained (CU)
   In a CU triaxial test, the soil sample is loaded to the required cell pressure where draining of the sample is allowed, so the sample is able to consolidate. After, the sample is loaded vertically until failure without drainage. One CU test provides one point in the Mohr stress space. A minimum of three tests are required at different cell pressures in order to determine the cohesion and friction angle of the soil sample. The influence of sampling disturbances is less with CU testing than for UU tests due to the pre-consolidation phase. The CU test is used to predict the shear resistance for cohesive and non cohesive soil samples. [15] The CU test can be separated into a

consolidated anisotropic undrained (CAU) test and a consolidated isotropic undrained (CIU) test, where the CAU is the most commonly used to provide data for test collections.

3. Consolidated drained (CD)
   The CD triaxial test first consolidates the soil sample by applying the cell pressure and allowing for drainage. After the consolidation process has ended, the sample is loaded vertically until the in-situ stress is reached or exceeding it, depending on the requirements. The test can provide drained and undrained parameters for cohesive soils.

4.3. Direct simple shear testing

The Direct Simple Shear (DSS) tests were added to the test collection of the Alblasserwaard after 2015. The DSS tests are used on peat samples since these cannot be tested in triaxial tests. The parameters resulting from the DSS testing can be applied in calculations using the SHANSEP method. The DSS test constrains the bottom and top of the soil sample and applies a horizontal displacement to simulate a shear load on the soil. The DSS test is useful to provide test data for normally consolidated (NC) or over-consolidated (OC) clays and peat soils.

The first stage of the DSS test is the consolidation phase, pre-loading of the sample to prevent swell from occurring in clay samples. The soil sample has a diameter between 50 to 70 mm and requires to be fully saturated for the test. The shearing of the sample can be done with a constant height constrain or a constant load on top of the sample. By using a constant sample height, the reaction of the sample will be undrained since there no volume change can occur. The horizontal deformation speed can be set at a constant speed of 1.6 mm/hour. The sample is known to have reached critical state at 40% straining. The peak shear stress is usually measured at 15% to 20% straining. For soils that have a lower consolidation stress than 20 kPa, extra precision during testing is required. [3]

DSS test	
Measurements before testing	A, e, θ
Measurements during testing	S_u, ε, σ'_v, Δu_w
Measurements after testing	A, e, θ, S_{u_p}, $S_{u_{cv}}$
Calculated parameters	ϕ_{cv}, ϕ_p, S_{cv}, S_p, OCR, m

Table 4.3: Direct simple shear test parameters

The parameters that are relevant in the DSS test are displayed in table 4.3. The parameters that can be calculated from that data are friction angle ϕ_{cv} at critical state, the peak friction angle ϕ_p, the shear strength ratio at critical state S_{cv} and the peak shear strength ratio S_p. [5]

4.4. Other laboratory tests

If more information is required on the soil behaviour or different parameters are requested to be determined, other soil laboratory tests can also be useful. Compression testing can provide information on the settlement behaviour of a soil or can be used if the primary and secondary compression coefficients are required. This test can also provide an estimate of the pre-consolidation stress of the soil type. With the introduction of the SHANSEP model, a new set of soil parameters was required to be determined. For example, by using a Constant Rate of Strain test (CRS), the Isotachen parameters can be extracted which determine the value for the exponent m. Additionally, the value for (isotropic) swell index κ and compression index λ can be calculated on the unloading and reloading curve output of the CRS. The POP can also be determined from this test. If a K_0-CRS test is used, the horizontal stress occurring in the soil sample can also be calculated. [3]

4.4.1. Comparison laboratory tests

The cell and triaxial test both use a cylindrical soil sample to deform the sample vertically in a similar matter. However, the cell test is performed by applying a vertical load, whilst the triaxial test sample is

loaded by applying a rate of strain. The cell pressure of the cell test cannot be fixed while performing the test, however can be lowered by removing the water from the cell space resulting in only drained testing. While the triaxial test can alter the cell pressures during the testing and perform drained and undrained analyses. From experience, it is also noted that with cell testing, the resulting shear strength of the soil is lower compared to the results of the triaxial tests. [10] If the shear strength is determined at small deformations of the test sample, which is the case for the cell test, the difference between the results will be large. The major difference between the two tests is that the shear strength of the soil sample will be determined at small strain (2 to 5 %) for cell tests, where the shear strength during a triaxial test is measured at failure (critical state) at large stain (20 to 25 %).

4.5. Test collection

Two main test collections can be distinguished:

- The test collection for the KIS reinforcement project
- The test collection for the SAFE project

Both test collections are added in Appendix B. The KIS test collection for the Alblasserwaard contains the test results from cell tests including an average value for the parameters c and ϕ per geological deposit. The collection includes $\sigma - \tau$ tables for each soil type, where the tables for sandy soils are assumed. The other $\sigma - \tau$ are directly measured from the cell testing. [7]

The test collection for project SAFE was set up in 2020 by using the WBI, triaxial tests and DSS laboratory tests were done from soil samples taken of the Lekdijk. These parameters are also used in the latest safety assessment for dike trajectory 16. The peat soils indicated in the test collection are tested by the DSS test and the other soils are tested with the triaxial test apparatus. The average and characteristic values for the SHANSEP model are documented in the test collection as well. A side note is that the m values for the clayey peat are considered unreliable.

4.5.1. Comparison test collections

The main difference between the two previously mentioned test collections is that the KIS test collection consists of cell test results and the SAFE collection of triaxial and DSS test results. The KIS collection contains the $\sigma - \tau$ curves for each soil type including the anthropogenic dike materials. The shear strength of each soil is given by a characteristic value and a design value, where for the zero value (cohesion) a material factor of 1.25 is applied and the general material factor (friction angle) of 1.15 is used. The SAFE collection includes the average value, characteristic value and the variation coefficient of each parameter. Note that the cell test provides the value of the drained shear strength of each soil and the triaxial and DSS tests are performed undrained and therefore provide undrained parameters. A fundamental change between the most recent test collections is the approach to different soil types. The SAFE test collections transitions to soil classification based on unit weight, not by geological deposit. The SAFE test collection is rewritten into the previously used soil type notation for consistency, which is included in appendix B.

The water autorithy is more experienced with the cell test collection since this collection has been used for years. The new test collection containing the triaxial and DSS test data, has just been set up in 2020. The development of this test collection is not yet complete. SAFE collection does include the variation in unit weight. The SAFE test collection does no longer distinguishes between O & N per soil layer, this is taken into consideration by the collection through the initial stress condition.

Another component that has not been taken into consideration is that between the laboratory test results and the test collection values, another material factor is used. Between the two collections, the material factors vary due to the uncertainties of different parameters influencing the safety standard differently. These material factors are most likely not the same for the cell test and the triaxial or the DSS test.

5

Modelling analysis

This chapter describes the process of determining the influence of the test collection and undrained modelling on the macro-stability safety assessment for dike profile AW159.+190m.

5.1. Macro-stability modelling software

The way in which the macro-stability of a dike profile is calculated has changed over the years. The modelling of macro-stability in the previous safety assessment for dike trajectory 16 is done in software provided by Deltares: D-Geo-Stability. In D-Geo-Stability, the shear strength model that is used to calculate the slope stability are stress tables. The values for cohesion and friction angle for each soil type are calculated from the $\sigma - \tau$ tables at the calculated effective normal stress value by using the Mohr-Coulomb model or $c - \phi$ model with dilatancy. Note that for the shear stress, characteristic values are used during the calculation process which describe the 5% lower limit. The MC model uses the definition $\tau = c + \sigma_n * \tan\phi$, if the dilatancy angle is assumed to be equal to the friction angle. [2] Since the stress table that is provided by the cell test results are determined at small strain, it is safe to assume that $\psi = \phi$. The model of this safety assessment in D-Geo-Stability is used to model the macro-stability of the dike cross-section AW159.+190m by using Bishop's method and UpliftVan.

The most recent macro-stability safety assessment follows the WBI, where D-Stability is used for the slope stability analysis with soft soils via Mohr-Coulomb, SHANSEP or using a S_u table. [6] In order to be able to compare the influence of the change in test collection, the model of the previous safety assessment is required to be transferred from D-Geo-Stability to D-Stability since it is not possible to perform undrained calculations from the SHANSEP formulation with D-Geo-Stability. Note that version 18.2.2 of D-Geo-Stability is used and version 2022.01.2 for D-Stability during the analysis.

5.2. Model transfer

A simplified model is used to assess the slope stability with one soil type in both software's to ensure that the transition to D-Stability of the previous assessment model in D-Geo-Stability is successful. Initially, the $\sigma - \tau$ tables were filled in the S_u table in D-Stability since this resembles the $\sigma - \tau$ table the most. If both the D-Geo-Stability and the D-Stability model provide the same value for the safety factor and the shear stress at three locations along the slip plane, the $\sigma - \tau$ table could be filled in the S_u table and the model can be transferred directly. The three locations to check the shear stress are chosen in the active, passive and horizontal section of the slip circle, and shown in figure 5.1. However, the simplified model does not give equivalent results with the S_u table. D-stability seems to overestimate the safety factor this process leads to difference in the shear strength. D-Geo-Stability assumes the $\sigma - \tau$ stress as normal effective stresses while the D-Stability S_u table interprets this input as vertical effective stresses.

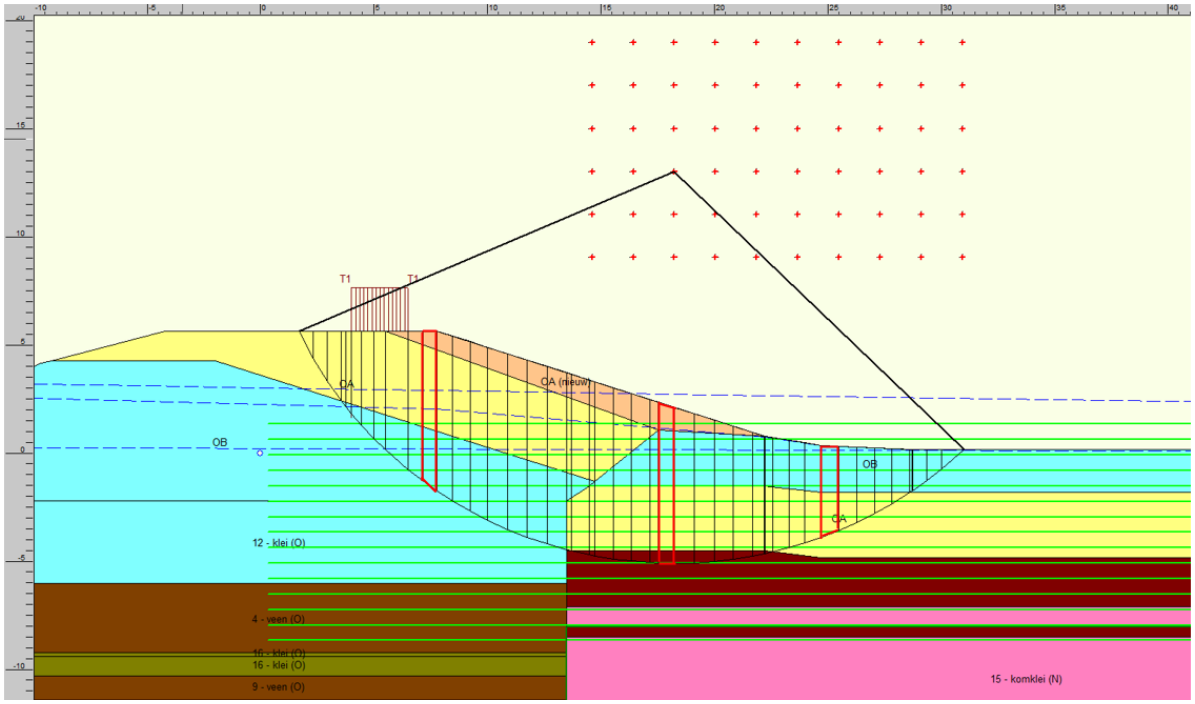

Figure 5.1: ADP Locations for Bishop slip surface

The most successful approach is calculate the equivalent values for c and ϕ via linear regression from each $\sigma - \tau$ table described in the test collection and use the Mohr-Coulomb drained calculation model. The method of approaching a value for c and ϕ does provide the same values in the simplified model for the safety factor, effective stresses and shear stress. This method is used to transfer the model to D-Stability.

5.2.1. Model constants

The provided D-Geo-Stability model for cross-section AW159.+190m is used as a base to determine the influence of the schematization of the shear strength. Many factors influence the value of the shear strength, these components will assumed to be constant, some of which are shown in table 5.1. The most critical slip circle is calculated in D-Geo-Stability by the original model with a brute force calculation for both Bishop and UpliftVan. The slip surface will be fixed in the other models.

Input parameters		
Crest height	5.65	m NAP
Average water level	0.33	m NAP
Design water level	3.55	m NAP
Traffic load	13.3	kN/m^2

Table 5.1: Constant input parameters for the calculation models

The D-Geo-Stability model uses the design values in the $\sigma - \tau$ tables to calculate the stability. To exclude the influence of any statistics, the model was adjusted to the characteristic values described in the test collection. The approach to determine the influence of changing the test collection is to adjust the model one step at a time to ensure a successful transfer to D-Stability. The modelling process is described in detail for both the Bishop calculation as well as the UpliftVan.

5.3. Bishop

Model 0: Original D-Geo-Stability Model

Model 0 is the original D-Geo-Stability model that was provided by WSRL to determine the safety factor for the dike profile AW159.+190m with Bishop's calculation method during the KIS reinforcement works. The model provides the critical slip surface with the lowest safety factor from an iterative calculation which is equal to 1.570. The only adjustment to this model is adjusting the $\sigma - \tau$ table from design to characteristic values, providing a new safety factor of 1.701. During the following stages of the process, the slip circle will be fixed.

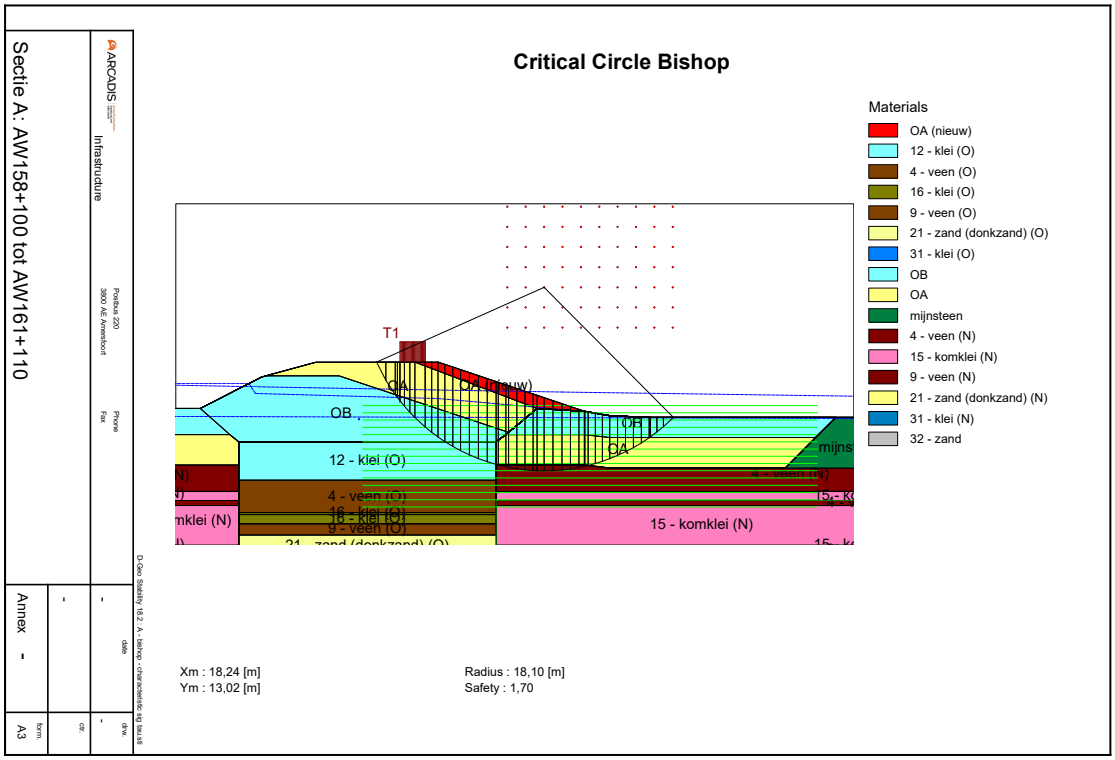

Figure 5.2: Result from D-Geo-Stability for model 0

The results for each model are documented in appendix D. The appendix includes a table that was used to document the resulting effective stresses, pore pressures and shear stress along the three points selected in the slip circle. During the process of transferring the model to D-Stability, it is important that these values remain constant.

Model 1: Extended $\sigma - \tau$ tables

The original model requires adjustment since the input $\sigma - \tau$ curves from the cell tests do not match the effective stress range in the subsoil. This was noticed during the modelling process due to the mismatch in values for the shear stress values in the horizontal section of the slip circle. The shear stress would be equal to the maximum shear strength in the $\sigma - \tau$ table, even if the effective stress at the location of the slice would be much higher. D-Geo-Stability does not extrapolate the shear stress values if the effective stress is higher than the σ from the $\sigma - \tau$ tables. It takes the highest value of shear strength provided in the table and uses that value for all locations where the effective stress exceeds the $\sigma - \tau$ table. It can be concluded that the provided model that was used in the previous safety assessment is not correct. The solution to this issue is to use D-Stability to extrapolate more

$\sigma - \tau$ points to extend the stress tables of the cell test collection. The process is as follows:

- From the original $\sigma - \tau$ tables, extract values for c and ϕ with a linear regression.
- Fill in these c and ϕ values in the D-Stability model and extract new $\sigma - \tau$ points for each soil where the range of the test collection does not suffice.
- Extend the $\sigma - \tau$ tables and add these to the original D-Geo-Stability model and document the results.

This provides more accurate shear stresses in the horizontal section of the slip surface. This procedure created model 1 and is now used as a base for the upcoming models. Due to this process, the safety factor is increased to 1.818.

Model 2: c and ϕ
The values for c and ϕ are calculated from the extended $\sigma - \tau$ tables via linear regression. The new values for c and ϕ are to be filled in the D-Geo-Stability model and the results are documented. The shear stress in the horizontal section of the slip circle is now more compatible to model 1 where only the extended $\sigma - \tau$ tables are used. The input of the D-Geo-Stability model with the adjusted values for c and ϕ is given in appendix C.

Model 3: Transfer to D-Stability
Model 2 can be transferred to D-Stability. The adjusted c and ϕ values are filled in the Mohr-Coulomb shear strength model, along with the unit weight of each soil. The water lines of the model required some adjustment. The results of model 3 in D-Stability match those of model 2, showing a successful export of the model.

Model 4: Undrained D-Stability
The model in D-Stability is adjusted to undrained SHANSEP parameters for the soft soils. The state of each soil layer is added to the model via the POP. During the modelling process, the volumetric weights are considered constant to isolate the effect of applying the SHANSEP parameters. The water level is modelled in multiple stages in D-Stability, where the everyday water level is modelled in the first stage and the second stage contains the design water level. The WBI is followed to indicate which soils should be modelled undrained and which should be considered drianed. The sandy soils are modelled using the MC-calculation model and the clay and peat soils with the SHANSEP formulation to simulate undrained behaviour. The input for this model is also given in appendix C.

Model 5: Free slip surface analysis
The last Bishop model is ran as undrained again, however with a free slip surface brute force analysis to determine the most critical slip surface under undrained conditions.

5.3.1. Results Bishop

A short summary of the stresses from the relevant Bishop models are displayed in table 5.2. Only the results for the models 3, the drained calculation with the characteristic and adjusted values for c and ϕ, model 4 the undrained SHANSEP calculation and model 5 with a brute force undrained Bishop calculation are shown in the table. All the results from each model is summarized in appendix D.

The initial model (0) was incorrect due to the limitation in applying the $\sigma - \tau$ tables. Higher consolidation stresses result in higher shear strengths. The problem only occurred in the horizontal section of the slip surface for a number of soils. However, this can also be classified as a conservative assumption to limit the shear strength to the maximum value provided in the $\sigma - \tau$ table. The increase in safety factor due to expanding the stress tables is however limited to 0.1 for Bishop and only 0.03 for the UpliftVan calculation.

Model	Slice	ADP Location	Effective stress [kN/m²]	Total pore pressure [kN/m²]	Shear stress [kN/m²]	Safety Factor [-]
3: Drained	11	Active	98.94	30.45	38.20	1.781
	27	Horizontal	75.70	56.72	34.00	
	40	Passive	36.34	38.93	27.82	
4: Undrained	11	Active	98.92	30.44	33.55	1.319
	29	Horizontal	75.70	56.72	27.32	
	42	Passive	37.04	40.48	11.64	
5: Free slip surface	14	Active	40.65	0	16.52	1.161
	24	Horizontal	40.94	29.82	14.19	
	36	Passive	16.01	21.18	5.29	

Table 5.2: Results Bishop drained vs undrained calculation

When comparing the factor of safety for model 3 (drained) and model 4 (undrained), the safety factor is decreased by 0.462. The shear stress around the slip surface has decreased, the largest decrease occurs in the passive section of the slip circle. The results of this calculation can not be used to determine the safety of the dike since the observed decrease in safety factor is not representative for the transition from the cell test collection to triaxial and DSS collection. The slip circle does not cross enough soil layers to gain a representative result. The most critical slip surface according to the model mostly crosses through the anthropogenic dike material. With performing a Bishop brute force calculation, the most critical slip surface changes. The circle radius decreases and only crosses the top dike material layers OA and OB. It is questionable if this could be considered as a macro-stability failure, since the remaining dike after sliding would still be able to retain water. Since the SHANSEP method is only applied on the soft soil layers and the sand soils are still modelled with the MC calculation method, the results for model 5 are considered unreliable.

5.4. UpliftVan

Model 6: Original D-Geo-Stability Model

Model 6 is the original D-Geo-Stability model that was used in the previous safety assessment to determine the stability via the UpliftVan calculation method for dike section AW158+100 to AW161+110. The most critical slip surface is determined and considered to be constant throughout the other models. The only adjustment to this model is to transfer the design values to characteristic values for the $\sigma - \tau$ table.

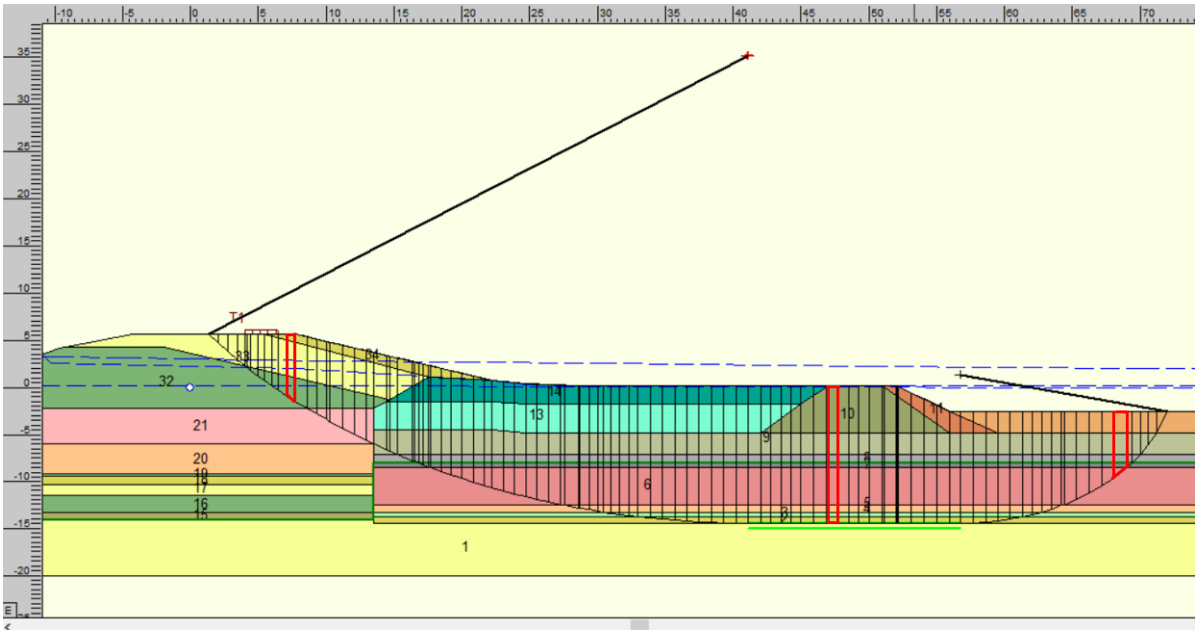

Figure 5.3: ADP Locations for UpliftVan slip surface

Figure 5.3 displays the locations from where the shear strength, effective stress and pore pressures will be documented. The same method that is applied for the Bishop analysis is used during the process of the UpliftVan calculations.

Model 7: Extended $\sigma - \tau$ tables & Model 8: c and ϕ values

Model 7 is the adjusted model in D-Geo-Stability with the extended $\sigma - \tau$ tables. The same values are used as for the Bishop calculation since the stress range remains the same. The adjusted c and ϕ values can be filled in the D-Geo-Stability model 8. The slip surface is kept constant throughout the models. It is ensured during the changes in models that the values for effective stress, pore pressures and shear stress remain constant along the slip surface.

Model 9: Transfer to D-Stability

Model 8 is transferred to D-Stability, creating model 9. To check if the search algorithm has changed for the UpliftVan failure mode, the most critical slip surface is determined in D-Stability by using the particle swarm calculation in model 9. This can be compared to a brute force calculation of model 8, so the most critical slip surfaces can be determined while the other parameters are kept constant. This process is not considered for the Bishop calculation since this model only takes a slip circle through the dike material when the brute force calculation method is used. The brute force calculations do not show the exact same slip surface, but they are highly comparable since the horizontal section runs through the same boundary with the Pleistocene sand.

Model 10: Undrained D-Stability model & Model 11: Free slip surface calculation

From model 9, the undrained UpliftVan model 10 is calculated by using the SHANSEP parameters from the SAFE test collection. The POP values are included in the model by assigning a state to each soil layer. The POP values for each soil layer is included in appendix C. The results are added in appendix D. With the calculation of free particle swarm UpliftVan the most critical slip surface is calculated for the undrained situation in model 11.

5.4.1. Results UpliftVan

The results from the UpliftVan models are shown in table 5.3. The decrease in safety factor of the drained (model 9) to undrained calculation (model 10) is equal to 0.12 which is in line with calculations that were executed during the first safety assessment. Due to this decrease, the dike profiles that were previously designed at the required safety factor of 1.17 for Uplift, will not suffice on the new macro-stability requirements.

Model	Slice	ADP Location	Effective stress [kN/m²]	Total pore pressure [kN/m²]	Shear stress [kN/m²]	Safety Factor [-]
9: Drained	12	Active	95.91	27.85	34.26	1.409
	77	Horizontal	60.07	163.27	23.53	
	106	Passive	8.59	88.90	8.20	
10: Undrained	12	Active	95.91	27.85	32.75	1.289
	78	Horizontal	60.07	163.27	24.71	
	109	Passive	12.56	88.90	5.12	
11: Free slip surface	14	Active	111.758	41.183	29.674	1.175
	80	Horizontal	60.019	163.891	21.193	
	104	Passive	11.909	140.656	6.005	

Table 5.3: Results Uplift drained vs undrained calculation

To highlight the influence of the transition from drained to undrained modelling, table 5.4 displays the difference in resulting shear stresses per slice around the slip surface. The table displays that there is a decrease in shear stress in almost all slices of the slip surface, with the exception of a number of slices in the horizontal section. The slip surface crosses the Pleistocene sand with the thin clay layer (31). This layer can also be modelled drained since the drainage length is short and the layer is enclosed by sandy soils. However, this layer is assumed to behave undrained since this soil is also known to be rigid and humus.

Soil type	Slice number drained	Slice number undrained	ADP Location	Drained shear stress [kN/m²]	Undrained shear stress [kN/m²]	Deviation
OA	2	2	Active	12.89	11.11	1.78
OB	12	12	Active	34.26	32.75	1.50
12. Clay O	16	16	Active	35.91	27.88	8.03
4. Peat N	20	20	Active	38.15	36.55	1.61
15. Komklei N	43	44	Active	24.96	20.00	4.96
9. Peat N	52	52	Horizontal	25.39	23.09	2.30
21. Donkzand N	56	56	Horizontal	29.33	29.13	0.20
31. Clay N	61	61	Horizontal	20.98	22.78	-1.80
Boundary 32. Sand	77	78	Horizontal	23.53	24.71	-1.18
31. Clay N	95	98	Passive	7.20	10.79	-3.59
21. Donkzand N	97	100	Passive	8.06	8.18	-0.12
9. Peat N	99	102	Passive	10.40	8.84	1.57
15. Komklei N	105	108	Passive	9.57	5.98	3.59
4. Peat N (in between 15)	107	110	Passive	8.14	2.41	5.72
4. Peat N	112	115	Passive	5.17	0.52	4.64

Table 5.4: Drained (model 9) vs undrained (model 10) shear strength in the UpliftVan calculation

In the particle swarm calculation of model 11 to determine the most critical slip surface in the undrained calculation, the failure surface does deviate from the critical failure surface determined in model 6. The circle radii decreases, however the horizontal slip plane is still located at the boundary of the Pleistocene sand, as can be seen in figure 5.4 .

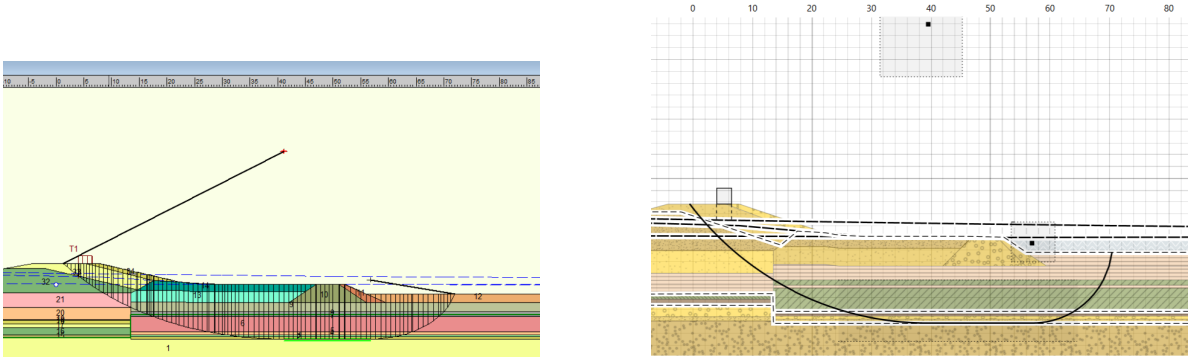

(a) Slip surface Uplift model 6: Original D-Geo-Stability Model

(b) Slip surface Uplift model 11: Free slip surface calculation

Figure 5.4: Critical slip surface comparison

It is proven to be difficult to create compare the test collections of the two safety assessments. There have been many changes in between the two macro-stability safety assessments so it has proven to be difficult to create a 'clean' comparison to isolate the influence of changing the test collections. The change in approach of both test collections in strength parameters c and ϕ are expected to have minor to no influence on the shear strength schematization. Since the triaxial test assume $c = 0$, but the values of ϕ are higher than in the cell tests, the stress range in the model will not lead to different values for the shear strength. However, the test collections are difficult to compare since the strength of the soils are determined at different values for strain.

The approach of comparing the two test collections by modelling the drained and undrained parameters of in D-Stability, has shown to work for the UpliftVan model. The process of approaching the $\sigma - \tau$ tables with a linear regression to determine the c and ϕ parameters for each soil type is successful. Models 7 and 8 show the transition from the stress tables to strength parameters for UpliftVan. The shear stresses occurring along the slip surface are equal for both models. The transition from D-Geo-Stability to D-Stability has also been validated, the shear stresses around the slip surface remain constant. It can be concluded that the transition from drained cell test parameters to undrained SHANSEP parameters resulted in a decrease in safety factor, where the shear strength around the slip surface also decreases.

6

Conclusion

In the previous safety assessment for inner slope macro-stability of the Lekdijk in the Alblasserwaard, $\sigma - \tau$ tables resulting from laboratory cell tests are used to indicate the shear strength of the dike material and soil layers. Multiple factors have been adjusted when comparing this macro-stability safety assessment to the most recent one performed in 2020 on cross-section AW159.+190m. Water levels have been adjusted, soil parameters, material factors, even the safety classification has changed, from a failure probability to a flooding probability.In the most recent safety assessment, the soft soil layers underneath the dike are considered to behave undrained and the SHANSEP formulation is used to model this behaviour. The method for modelling the inner slope stability has been extended over time. From only performing Bishop calculations with a fixed slip circle to using software to determine the most critical slip surface. Both safety assessments can be compared by isolating each component that influences the macro-stability of the dike profile. The most influential factors between the two safety assessments are expected to be the change of test collections from cell testing to triaxial testing and the drained to undrained modelling of the slope stability.

The test collections that are used in modelling the inner slope macro-stability of the dike has transitioned from a cell test collection to a triaxial test and DSS test collection. According to the ADP method, the slip circle resulting from a macro-instability can be divided into three sections: an active, horizontal and passive section. In theory, the triaxial compression test is most suitable to simulate the loading conditions in the active section of the slip circle, where the triaxial extension test simulates the loading conditions in the passive section. The horizontal segment is best simulated with a direct simple shear test. In practice, the triaxial compression tests are used to determine the shear strength of clay soil samples. The direct simple shear test is used to provide the shear strength of peat soils, since triaxial test on peat soils provide unreliable results due to high straining.

The cell tests provide $\sigma - \tau$ tables for each soil type, from where the Mohr-Coulomb formulation can be used to define values for the cohesion c and friction angle ϕ. The triaxial tests friction angle is determined at critical state where the cohesion is assumed to be zero. It is difficult to compare the cell and triaxial tests since the strength parameters are determined at 2 to 5% strain for cell testing and at 20 to 25% stain. Both laboratory tests provide $\sigma - \tau$ correlations, from which the strength parameters are determined. When only drained versus undrained parameters in the test collections are considered, it is best to exclude the change in volumetric weight of each soil. To provide a clean comparison, only the calculation model is changed from MC with parameters c&ϕ, to the SHANSEP calculation model including parameters S, m&POP. The influence of undrained modelling of the shear strength can be visualised by modelling a dike cross-section in D-Stability and use the MC calculation for a drained analysis and SHANSEP for an undrained analysis. Other factors and components are to remain constant. The MC parameters are extracted from the $\sigma - \tau$ tables provided by the cell test collection by linear regression. The SHANSEP parameters are extracted from the SAFE test collection.

The dike cross-section AW159.+190m is modelled in D-Stability with the cell test collection and triaxial and DSS test collection to analyse the influence of the change in test collection. The safety factor

for a Bishop calculation decreases with 0.5, and for the UpliftVan calculation there is a decrease of 0.12. It can be concluded that the change in test collection results in a decrease in safety factor when modelling the macro-stability of the dike cross section. The Bishop calculation however, is deemed unreliable since the slip circle only includes dike material, and therefore is not representative. The parameters describing this material are mostly based on assumptions. The UpliftVan model is in line with the expectations of the WSRL. It can be concluded that the transition to a different test collection, with the undrained modelling of the shear stress results in a decrease of the safety factor. The average decrease in safety factor is equal to 0.12 with a large standard deviation.

7

Recommendation

The method of approaching the values for c&ϕ from the $\sigma - \tau$tables by a linear regression could be improved by schematizing the values for c&ϕ in sections. Section one can describe the soil behaviour until the peak strength is reached, and section 2 can describe the soil behaviour at critical state. This can improve the model transfer from D-Geo-Stability to D-Stability. This can also account for the limitation of the $\sigma - \tau$ tables that are used during the previous safety assessment. However, more data points are required in the cell stress tables.

To ensure validity of the results that the safety factor decreases due to the transition in test collection, more cross-sections of the Lekdijk should be investigated.

The model in D-Stability can be improved by investigating the accuracy of the geometry and soil lithology of the current geometry. By using recent CPT data, the schematization of the subsoil can be checked and optimized.

Another improvement that is required to the investigation method is to investigate the statistical process of transferring the laboratory test results to the characteristic values described in the test collection. It is likely that there is another material factor that was used, which are not equal for the different laboratory tests. This process is not taken into consideration, however can impact the outcome of the analysis. This could be investigated by comparing the standard deviation on the characteristic values mentioned in both test collections.

Probabilistic calculation methods can be used to better approach the actual safety of the dike cross-section. Stochastic parameters can be assigned in D-Stability that are expected to have great influence on the factor of safety. A sensitivity analysis can be used to highlight the differences in safety factor by comparing two components.

Further steps that can be taken to determine the influence of schematization of the shear strength on the safety assessment for macro-stability is to investigate the influence of the change in safety norms. The transition from a failure probability to a flooding probability is expected to have had a major influence on the safety assessment of the macro-stability of a dike, according to multiple experts in the field. It is still unsure what the magnitude of this change is.

References

[1] Jan Blinde and Alexander van Duinen. *Personal communication*. Mar. 2023.

[2] Deltares. *D-Geo Stability User Manual*. Tech. rep. Delft: Deltares, Sept. 2020.

[3] dr. G. Greeuw, drs. H.M. van Essen, and ing. T. A. van Duinen. *Protocol laboratoriumproeven voor grondonderzoek aan waterkeringen*. Tech. rep. Delft: Deltares, May 2016.

[4] S N Jonkman et al. *Flood Defences Lecture notes CIE5314*. Tech. rep. 2021.

[5] Leo Kwakman. *Regionale Proevenverzameling Beschrijving Parameters*. Tech. rep. Hoorn: Arcadis, Feb. 2016. URL: www.arcadis.com.

[6] R. van der Meij. *D-Stability User Manual*. Tech. rep. Delft: Deltares, Sept. 2020.

[7] W B Ponsteen and J Tigchelaar. *Analysetool SHANSEP STOWA-database-proevenverzameling 4.2*. Tech. rep. Hoogheemraadschap van Delfland, Apr. 2016.

[8] Water Verkeer en Leefomgeving Rijkswaterstaat. *Schematiseringshandleiding macrostabiliteit WBI 2017*. Tech. rep. Rijkswaterstaat, Nov. 2019. URL: www.helpdeskwater.nl.

[9] Technische Adviescommissie voor de Waterkeringen. *Leidraad voor het ontwerpen van rivierdijken deel 1*. Tech. rep. 's-Gravenhage: Staatsuitgeverij, Sept. 1985.

[10] Technische Adviescommissie voor de Waterkeringen. *Technisch Rapport Waterkerende Grondconstructies; Geotechnische aspecten van dijken, dammen en boezemkaden (in Dutch)*. Tech. rep. 2001.

[11] Technische Adviescommissie voor de Waterkeringen. *TR Leidraad cel en triaxiaalproeven*. Tech. rep. Oct. 1988.

[12] Technische adviescommissie voor de waterkeringen. *Leidraad voor het ontwerpen van rivierdijken deel 2-benedenrivierengebied*. Tech. rep. 's-Gravenhage, Sept. 1989.

[13] Jan Tigchelaar. *Personal communication*. Lelystad, Mar. 2023.

[14] Unesco Nederlandse Commissie. *Unesco | Molens van Kinderdijk-Elshout*. URL: https://www.unesco.nl/nl/erfgoed/molens-van-kinderdijk-elshout.

[15] Arnold Verruijt. *Grondmechanica*. 2001.

[16] Waterschap Rivierenland. *De Bosatlas van de Alblasserwaard*. Ed. by Waterschap Rivierenland. first. June 2017.

A

Appendix I. Local stratigraphy

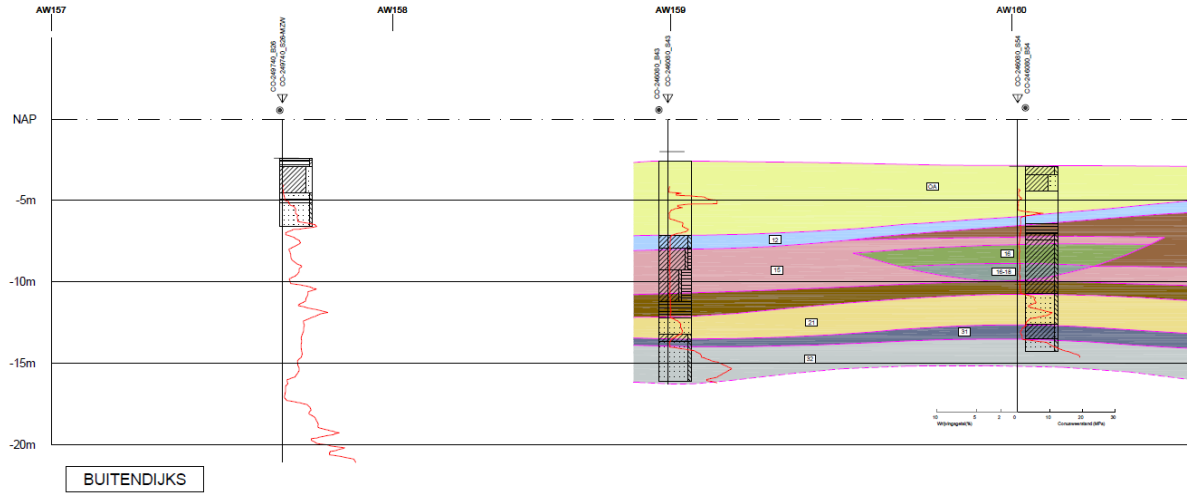

Figure A.1: Profile of the local stratigraphy underneath the outer slope of the dike from AW158 to AW160

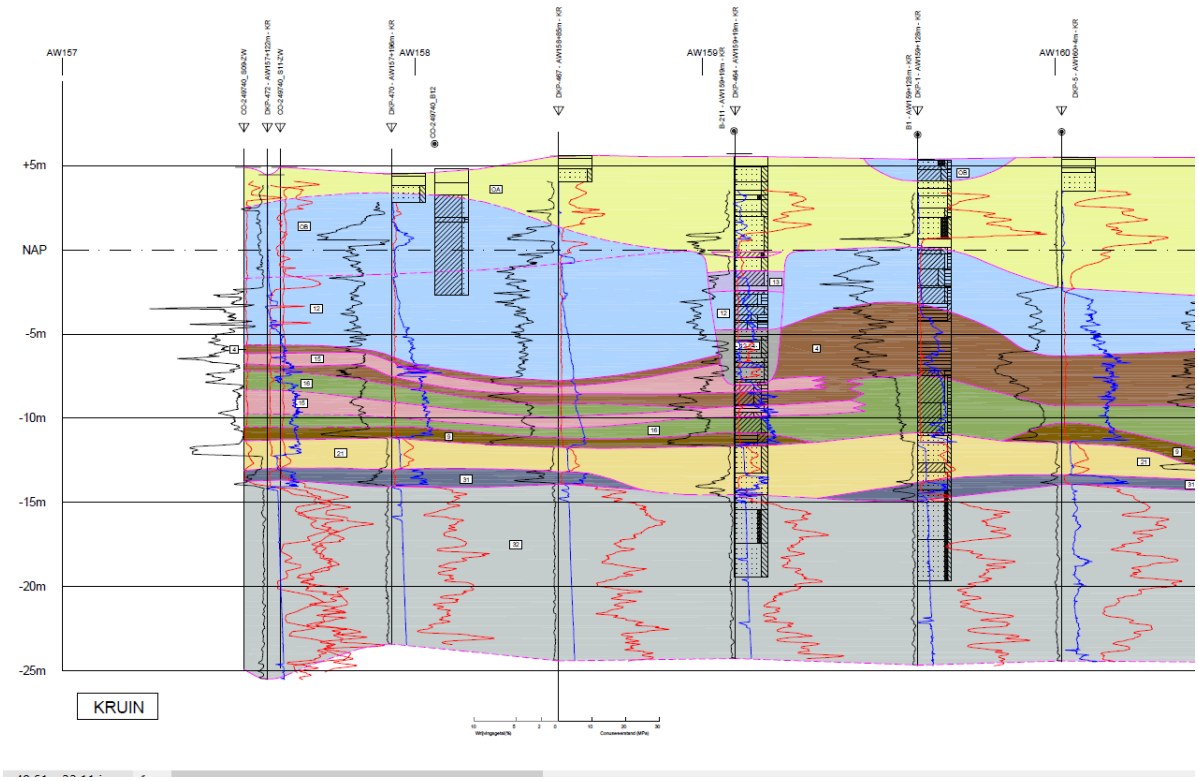

Figure A.2: Profile of the local stratigraphy underneath the dike crest from AW158 to AW160

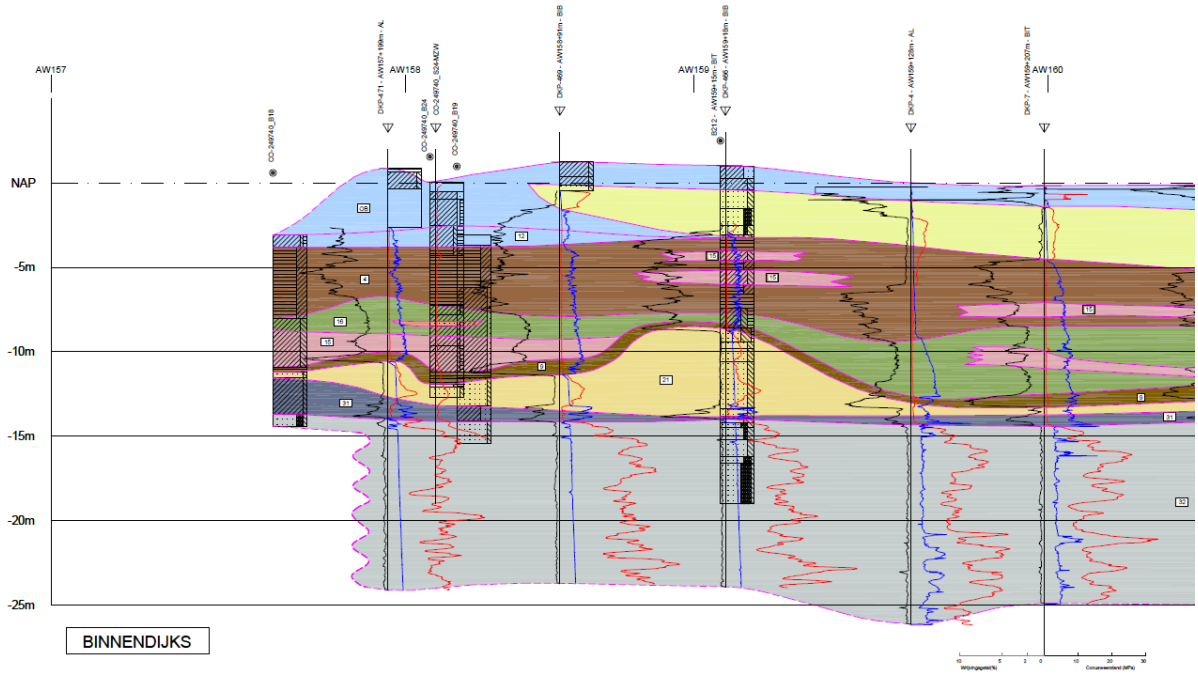

Figure A.3: Profile of the local stratigraphy underneath the inner dike section at dike pole AW158 to AW160

B

Appendix II. Test collections

B.1. Test collection KIS

Soil	**Soil description**	**WBI notation**	**Dry unit weight [kN/m³]**	**Saturated unit weight [kN/m³]**	**Average unit weight [kN/m³]**
Dike material	OA	-	17.2	19.2	17.2
Dike material	OB	-	15.5	16.0	15.5
15. Gorkum klei licht	Clay ('Komklei')	H_Rk_k&v	13.5	13.5	13.24
16. Gorkum klei zwaar	Sandy clay	H_Ro_z&k	17.1	19.1	16.78
12. Tiel klei	Clay interlayered with sand	H_Ro_z&k	17.1	17.1	17.07
4. Hollandveen	Peat	H_Vhv_v	10.9	10.9	10.89
9. Basisveen	Compacted peat	H_Vbv_v	11.6	11.6	11.38
14. Sand	Sand, locally with peat or clay	H_Rg_mf	17.1	19.1	17.1
17. Clay	Clay interlayered with sand	H_Ro_z&k	17.1	17.1	17.76
31. PL Sandy clay	Silty sandy clay	P_Rk_k&s	17.5	17.5	17.66
32. PL Sand	Sand. fine to medium	P_Rg_zm	18.0	20.0	18.0

Table B.1: Volumetric weight per soil from KIS test collection

$\sigma - \tau$ table 32. Sand $[kN/m^2]$		
σ	τ_{design}	$\tau_{characteristic}$
0	0	0
200	115.47	115.47

Table B.2: $\sigma - \tau$ 32. Sand

$\sigma - \tau$ table Mijnsteen $[kN/m^2]$		
σ	τ_{design}	$\tau_{characteristic}$
0	0	0
200	140.05	140.05

Table B.3: $\sigma - \tau$ Mijnsteen

$\sigma - \tau$ table OA $[kN/m^2]$		
σ	τ_{design}	$\tau_{characteristic}$
0	0	0
200	129.88	129.88

Table B.4: $\sigma - \tau$ OA

$\sigma - \tau$ table OA New $[kN/m^2]$		
σ	τ_{design}	$\tau_{characteristic}$
0	2	0
200	91.05	91.05

Table B.5: $\sigma - \tau$ OA New

$\sigma - \tau$ table OB $[kN/m^2]$		
σ	τ_{design}	$\tau_{characteristic}$
0	2.05	2.56
13	8.05	9.16
26	13.78	15.46
39	18.95	21.16
52	23.58	26.25
65	28.10	31.22
78	33.16	36.78
91	37.29	41.32
104	41.03	45.44
110.5	44.60	49.37

Table B.6: $\sigma - \tau$ OB

$\sigma - \tau$ table 31 Clay $[kN/m^2]$	
σ	$\tau_{characteristic}$
0	0.96
10	5.15
20	9.60
30	13.74
40	17.68
60	24.82
70	27.90
80	30.90
90	34.51

Table B.7: $\sigma - \tau$ 31 Clay

$\sigma - \tau$ table Peat 4 & 9 N $[kN/m^2]$		
σ	τ_{design}	$\tau_{characteristic}$
0	0	0
7	4.44	5.04
14	8.15	9.3
21	11.25	12.88
28	16.44	16.03
35	13.99	18.84
42	18.46	21.17
49	21.48	24.63
56	22.96	26.34
59	24.59	28.21

Table B.8: $\sigma - \tau$ table Peat 4 & 9 N

$\sigma - \tau$ table Peat 4 & 9 O $[kN/m^2]$		
σ	τ_{design}	$\tau_{characteristic}$
0	0	0
12	16.22	18.23
24	24.96	28.28
36	32.12	36.52
48	37.20	42.36
60	42.17	48.07
72	45.14	51.49
84	51.32	58.6

Table B.9: $\sigma - \tau$ table Peat 4 & 9 O

$\sigma - \tau$ table Tiel N $[kN/m^2]$		
σ	τ_{design}	$\tau_{characteristic}$
0	0.67	0.84
11	6.07	6.78
22	10.25	11.37
33	14.28	15.81
44	18.45	20.40
55	21.80	24.08
66	25.64	28.30
77	29.69	32.76
88	34.01	37.51
99	38.60	42.56

Table B.10: $\sigma - \tau$ Tiel N

$\sigma - \tau$ table Tiel O $[kN/m^2]$		
σ	τ_{design}	$\tau_{characteristic}$
0	0.65	0.82
12	6.50	7.24
24	11.45	12.69
36	15.74	17.42
48	19.29	21.32
60	22.87	25.25
72	27.24	30.06
84	33.63	37.10
96	37.09	40.90
108	42.07	46.37

Table B.11: $\sigma - \tau$ Tiel O

$\sigma - \tau$ table 16. Heavy Gorkum clay N $[kN/m^2]$		
σ	τ_{design}	$\tau_{characteristic}$
0	1.14	1.42
12	6.09	6.87
24	10.84	12.09
36	15.06	16.74
48	18.92	20.99
60	23.02	25.49
72	27.17	30.06
84	30.79	34.03
96	34.30	37.91
114	38.84	42.90

Table B.12: $\sigma - \tau$ 16. Heavy Gorkum clay N

$\sigma - \tau$ 16. Heavy Gorkum clay O $[kN/m^2]$		
σ	τ_{design}	$\tau_{characteristic}$
0	2.78	3.48
12	9.80	11.20
24	15.83	17.83
36	21.01	23.53
60	29.81	33.21
72	33.24	36.98
84	36.90	41.01
96	40.68	45.17
108	44.60	49.48
120	46.90	52.00

Table B.13: $\sigma - \tau$ 16. Heavy Gorkum clay O

$\sigma - \tau$ table 16. Light Gorkum clay N $[kN/m^2]$		
σ	τ_{design}	$\tau_{characteristic}$
0	1.52	1.90
12	6.76	7.66
24	11.16	12.50
36	15.14	16.89
48	18.69	20.79
60	22.84	25.35
72	23.83	26.44
84	28.17	31.22
90	32.50	34.88

Table B.14: $\sigma - \tau$ 16. Light Gorkum clay N

$\sigma - \tau$ 16. Light Gorkum clay O $[kN/m^2]$		
σ	τ_{design}	$\tau_{characteristic}$
0	1.95	2.44
14	13.29	14.91
28	20.10	22.40
42	25.76	28.63
56	30.47	33.81
70	34.28	38.01
84	38.00	42.10
98	40.55	44.90

Table B.15: $\sigma - \tau$ 16. Light Gorkum clay O

B.2. Test collection SAFE

WBI	Dry unit weight [kN/m³]	Sat unit weight [kN/m³]	Water con-tent [%]	Test	Number	Friction angle [°]	S[-]	m[-]	POP
OA	17	19	-	-	-	30	-	-	-
OB	17	17	-	-	-	27	-	-	-
OA New	14.98	19.04	-	TX	7	29.4	0.32	0.71	7
H_Vhv_v	2.86	10.3	294	DSS	36	29.8	0.34	0.78	1
H_Vbv_v	12	12	-	DSS	12	29.3	0.31	0.8	15
H_Rk_ko & H_Rk_k&v	5.91	13.08	125	TX	12	38.1	0.26	0.84	15
H_Ro_z&k_k	11.64	16.82	45	TX	29	30.3	0.22	0.95	15
P_Rk_k&s	14.61	18.73	29	TX	20	31.4	0.26	0.97	15
P_Rg_Zg	18	20	-	-	-	31.3	-	-	-

Table B.16: Characteristic values of

C

Appendix III.D-Geo-Stability & D-Stability input

Input D-Geo-Stability model (drained) characteristic values					
D-Stability AW159_Drained	c [kPa]	phi [°]	psi [°]	Dry unit weight [kN/m³]	Saturated unit weight [kN/m³]
OB dike material	4.125	22.318	22.318	17.5	17.5
Mijnsteen	0.000	35.004	35.004	18.0	20.0
OA	0.000	33.000	33.000	18.0	20.0
OA new	2.000	24.003	24.003	18.0	20.0
31. Clay Kreftenheye N	2.827	19.019	19.019	19.0	19.0
31. Clay Kreftenheye O	2.827	19.019	19.019	20.2	20.2
4. Hollandveen N	3.691	21.915	21.915	10.5	10.5
4. Hollandveen O	8.706	32.481	32.481	12.5	12.5
9. Peat N	3.691	21.915	21.915	10.3	10.3
9. Peat O	8.706	32.481	32.481	11.5	11.5
15. Clay Gorkum light N	3.504	19.626	19.626	13.0	13.0
15. Clay Gorkum light O	8.184	22.421	22.421	-	-
16. Clay Gorkum heavy O	7.533	21.122	21.122	16.4	16.4
16. Clay Gorkum heavy N	2.902	20.067	20.067	-	-
12. Clay Tiel N	1.895	22.146	22.146	-	-
12. Clay Tiel O	3.095	20.692	20.692	18.0	18.0
21. Donkzand O	0.000	30.000	30.000	21.0	21.0
21. Donkzand N	0.000	30.000	30.000	21.0	21.0
32. Sand	0.000	30.002	30.002	19.1	19.1

Table C.1: Input values for the D-Geo-Stability model (only characteristic values)

Input D-Stability Undrained SHANSEP characteristic values						
D-Stability_Char_Undrained	Dry unit weight [kN/m³]	Saturated unit weight [kN/m³]	S[-]	m[-]	POP[kPa]	Friction angle [°]
OB	17.5	17.5	0.31	0.8	-	27
Mijnsteen	18	20	-	-	-	30
OA	18	20	-	-	-	30
OA new	18	20	-	-	-	29.4
31. Clay Kreftenheye N	19	19	0.26	0.97	15	31.4
31. Clay Kreftenheye O	20.2	20.2	0.26	0.97	15	31.4
4. Hollandveen N	10.5	10.5	0.34	0.78	1	29.8
4. Hollandveen O	12.5	12.5	0.34	0.78	1	29.8
9. Peat N	10.3	10.3	0.31	0.8	15	29.3
9. Peat O	11.5	11.5	0.31	0.8	15	29.3
15. Clay Gorkum light N	13	13	0.26	0.84	15	38.1
15. Clay Gorkum light O	-	-	0.26	0.84	15	38.1
16. Clay Gorkum heavy O	16.4	16.4	0.26	0.84	15	38.1
16. Clay Gorkum heavy N	-	-	0.26	0.84	15	38.1
12. Clay Tiel O	18	18	0.22	0.95	15	30.3
21. Donkzand O	21	21	-	-	15	31.4
21. Donkzand N	21	21	-	-	15	31.4
32. Sand	19.1	19.1	-	-	-	31.3

Table C.2: Characteristic SHANSEP parameters input D-Stability

D

Appendix IV. D-Geo-Stability & D-Stability results

D.1. Results models Bishop calculation

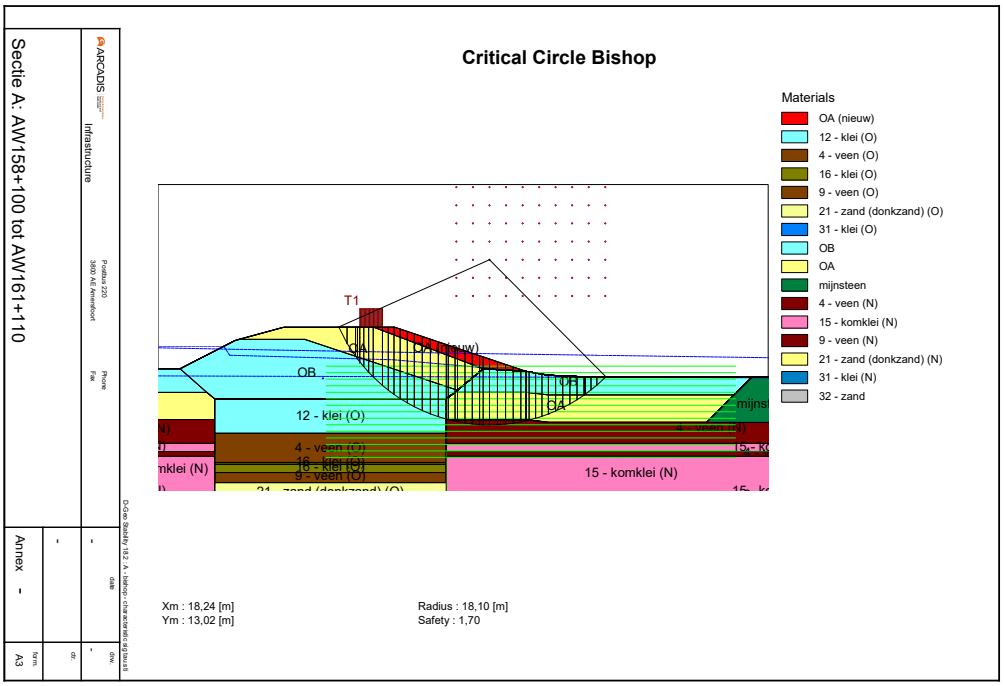

Figure D.1: Results model 0: Original D-Geo-Stability model, characteristic values

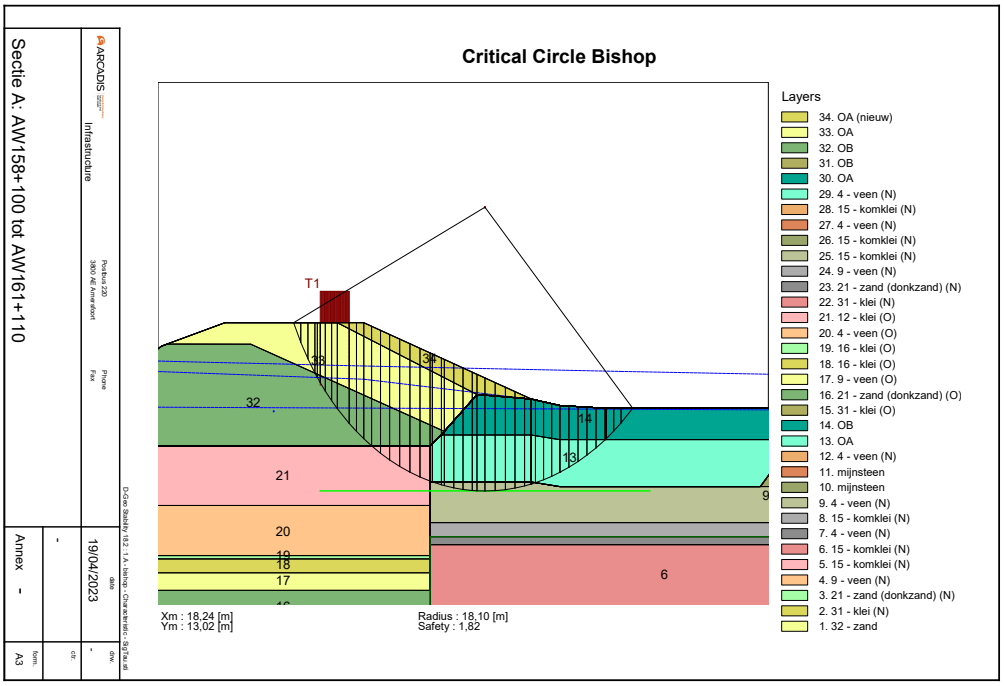

Figure D.2: Results model 1: Adjusted $\sigma - \tau$ tables

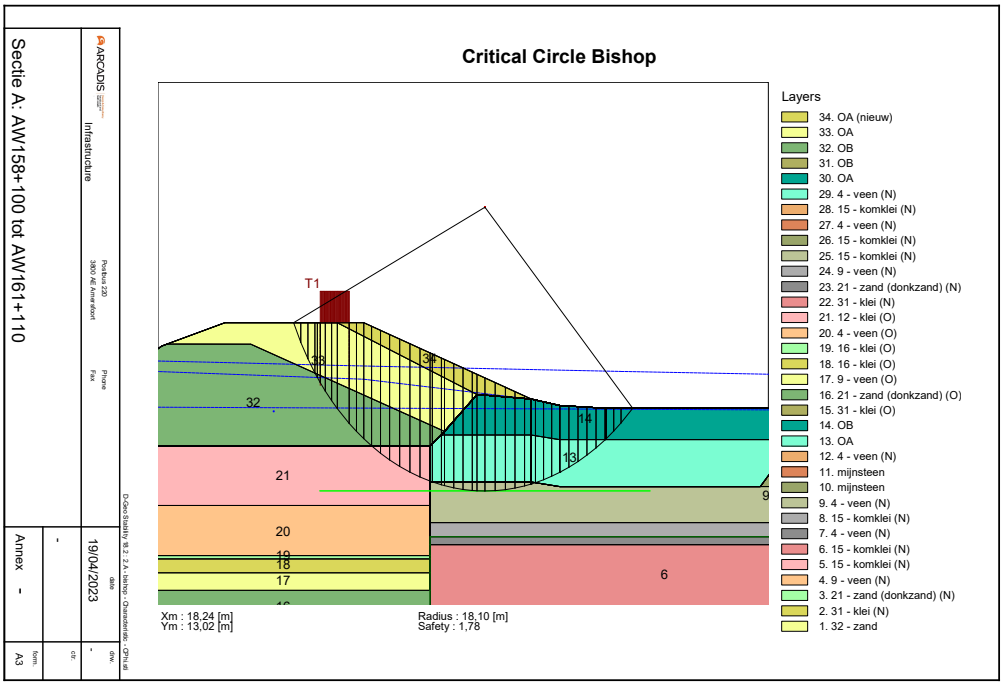

Figure D.3: Results model 2: C and Phi model

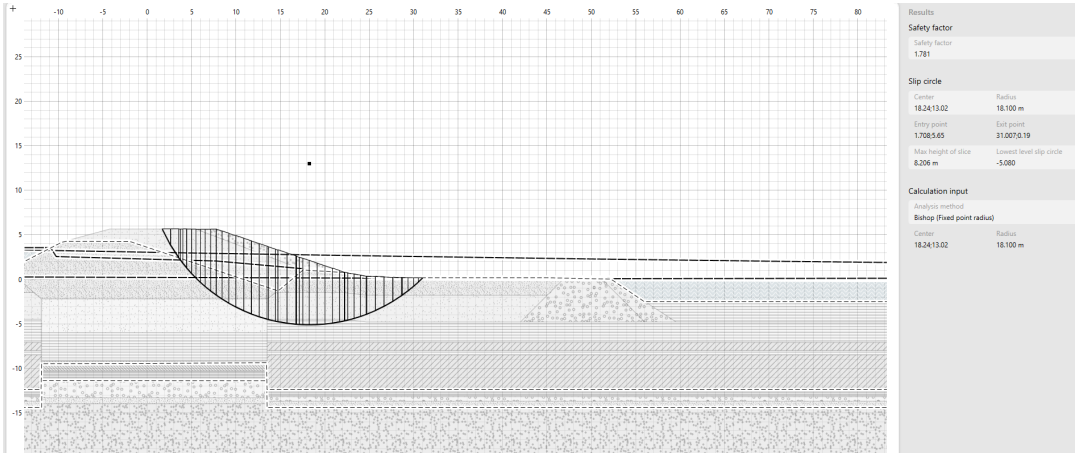

Figure D.4: Results model 3: D-stability transfer

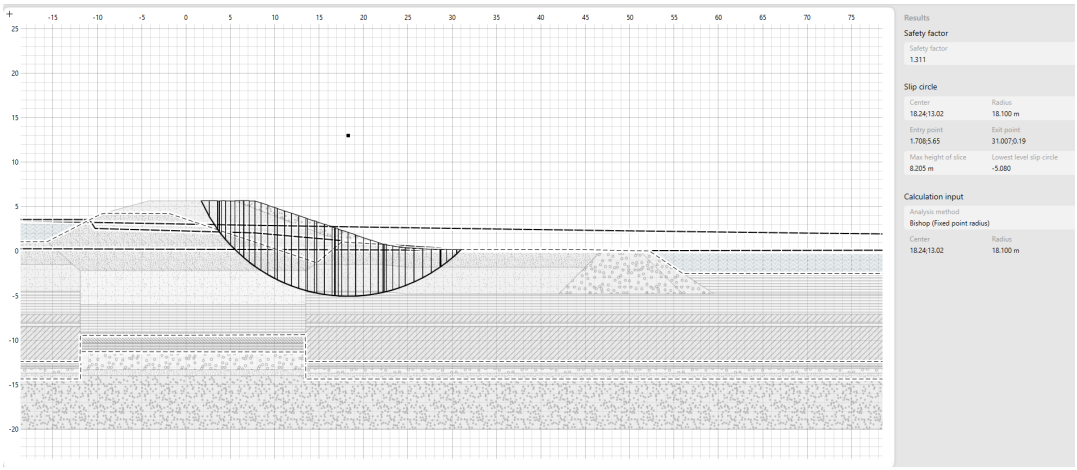

Figure D.5: Results model 4: Undrained D-Stability analysis

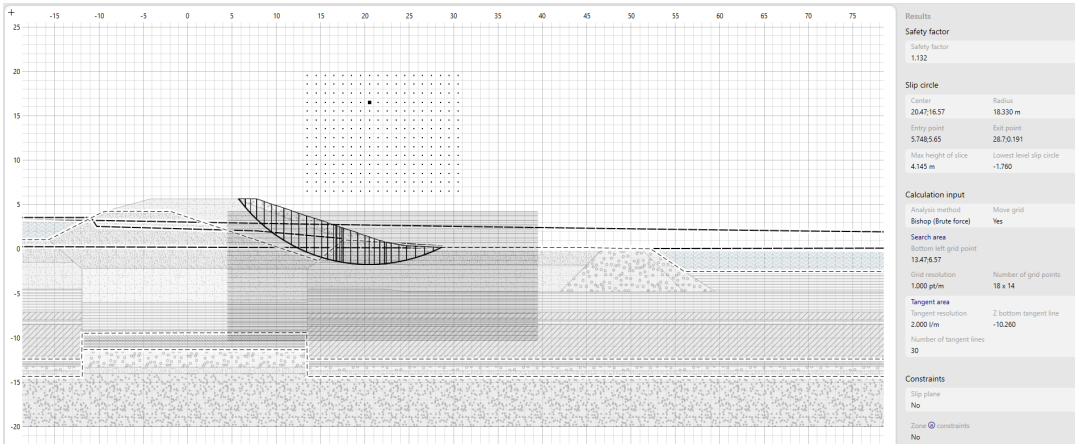

Figure D.6: Results model 5: Brute force Bishop calculation

D.2. Results models Uplift calculation

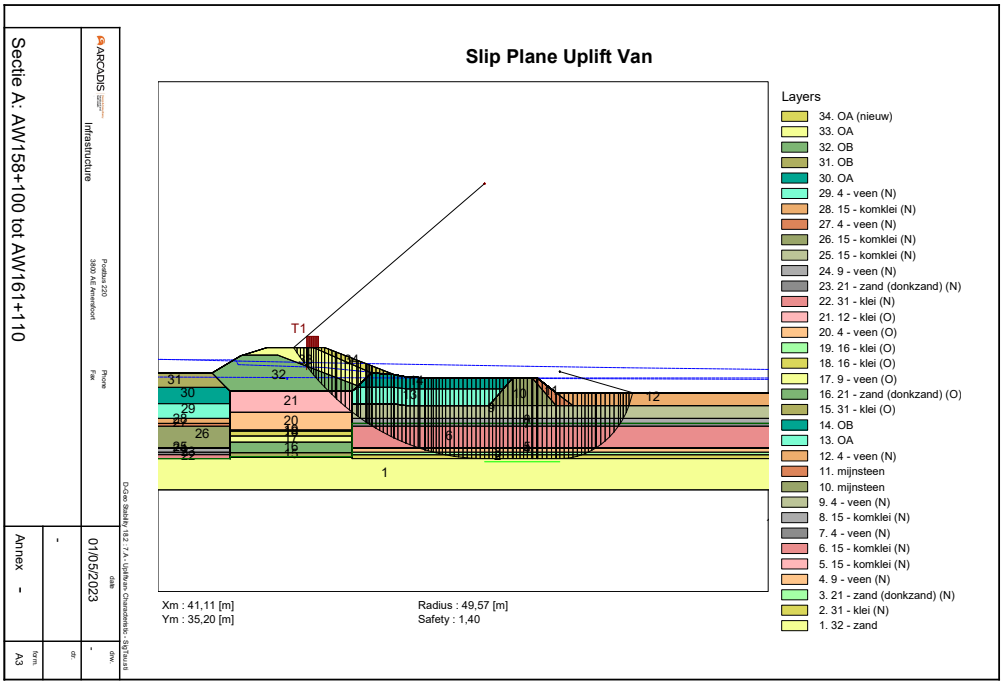

Figure D.7: Results model 6: Original D-Geo-Stability model for UpliftVan

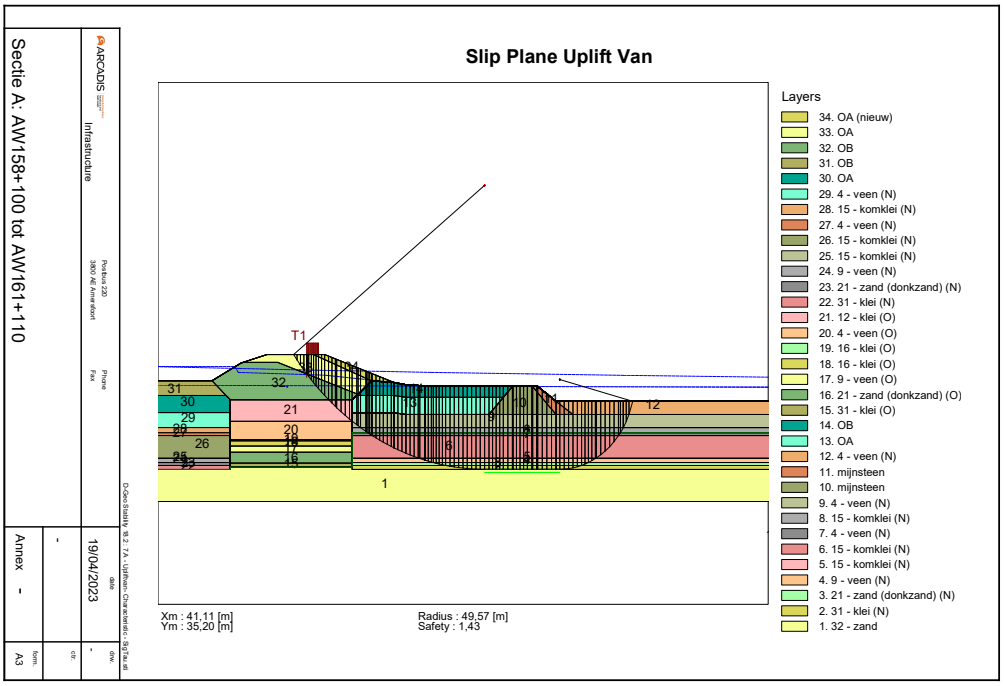

Figure D.8: Results model 7: Adjusted $\sigma - \tau$ tables

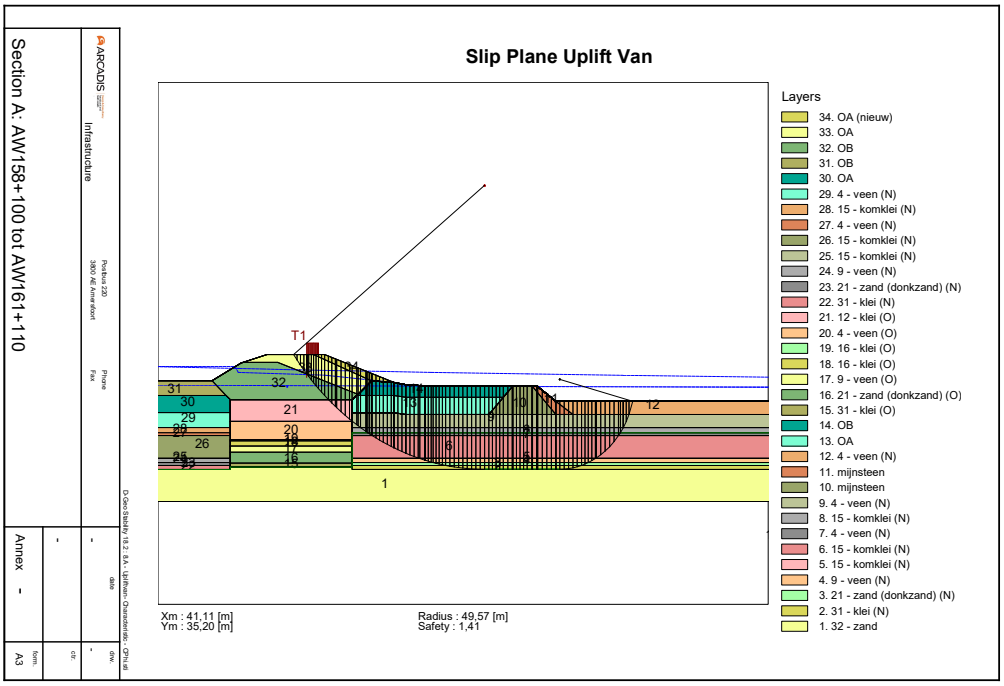

Figure D.9: Results model 8: C and Phi model

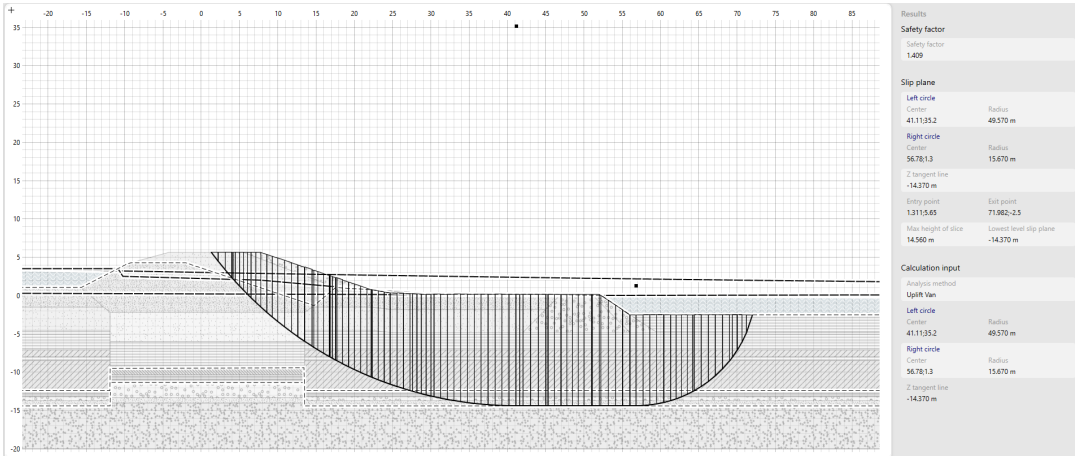

Figure D.10: Results model 9: D-stability transfer

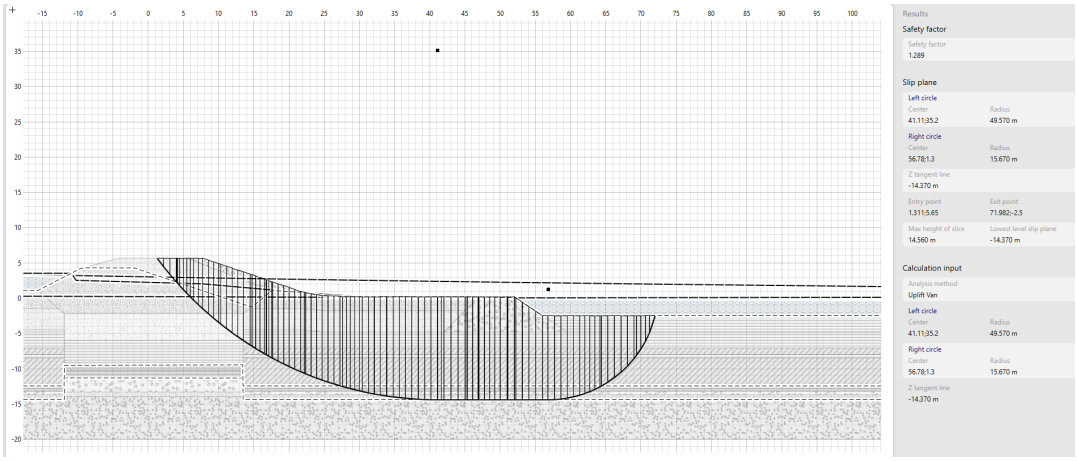

Figure D.11: Results model 10: Undrained D-Stability analysis

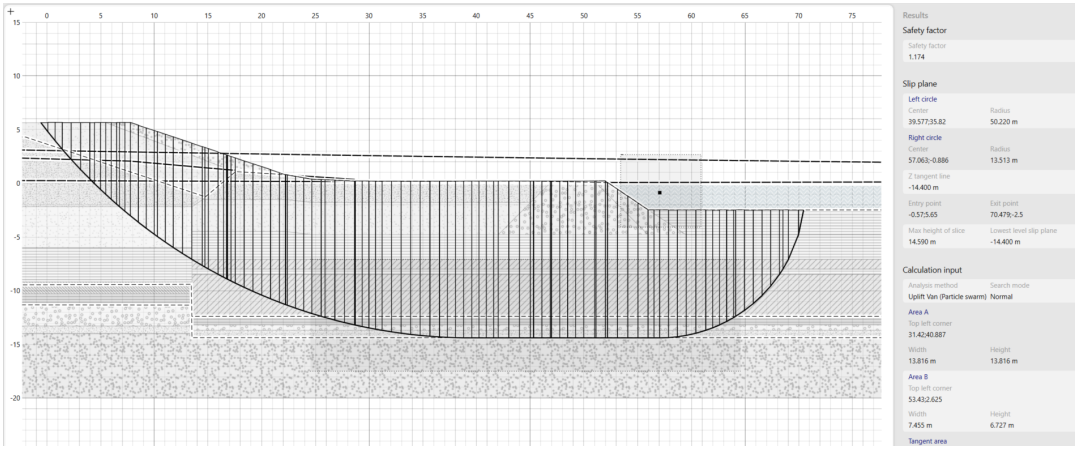

Figure D.12: Results model 11: UpliftVan particle swarm

D.3. Model comparison

Model	Slice	ADP location	Effective stress [kN/m²]	Total pore pressure [kN/m²]	Shear stress [kN/m²]
0	10	Active	98.913	30.412	34.816
	25	Horizontal	75.696	56.675	24.59
	38	Passive	36.866	39.153	28.848
1	11	Active	98.943	30.438	38.815
	26	Horizontal	75.692	56.723	36.089
	39	Passive	36.943	39.225	28.102
2	11	Active	98.948	30.442	38.213
	26	Horizontal	75.695	56.724	33.988
	39	Passive	36.937	39.224	28.2
3	11	Active	98.940	30.454	38.204
	27	Horizontal	75.695	56.724	33.997
	40	Passive	36.337	38.925	27.818
4	11	Active	98.920	30.438	33.552
	29	Horizontal	75.695	56.724	27.324
	42	Passive	37.039	40.476	11.635
5	4	Active	40.646	0	16.516
	24	Horizontal	40.939	29.824	14.194
	36	Passive	16.01	21.182	5.287

Table D.1: Comparison Bishop models

Model	Slice	ADP location	Effective stress [kN/m²]	Total pore pressure [kN/m²]	Shear stress [kN/m²]
6	13	Active	96.207	28.086	31.562
	76	Horizontal	60.006	163.893	24.806
	108	Passive	8.986	89.094	7.172
7	13	Active	95.955	27.87	34.803
	76	Horizontal	60.058	163.271	24.832
	108	Passive	8.988	89.103	8.196
8	13	Active	95.946	27.863	34.309
	76	Horizontal	60.058	163.271	23.537
	108	Passive	8.988	89.102	8.348
9	12	Active	95.914	27.852	34.261
	77	Horizontal	60.071	163.271	23.533
	106	Passive	8.587	88.896	8.178
10	12	Active	95.914	27.852	32.752
	78	Horizontal	60.071	163.271	24.708
	109	Passive	12.561	88.896	5.121
11	14	Active	111.758	41.183	29.674
	80	Horizontal	60.019	163.891	21.193
	104	Passive	11.909	140.656	6.005

Table D.2: Comparison Uplift models